Treball de Fi de Master

Mobility Incoming

Simulation study of integrated tandems of kesterite/c-Si solar cells

MEMÒRIA

Autor: Roberto Micari
Director: Santiago Silvestre Bergés

Convocatòria: July 2018

Escola Tècnica Superior
d'Enginyeria Industrial de Barcelona

Abstract

During the last years, the words “energy transition” have been very common. This sentence means that people interested in the field of energy production are looking forward non-conventional power generation sources, in substitution of conventional fossil fuel power sources, in order to satisfy the society needs in terms of energy demand. In addition, governments and international organizations (i.e. the European Union) are developing programs and fixing targets aimed to speed up this energy transition. They are some of the reasons why renewable energy technologies are experiencing a fast growth. Among the several ones, this work focuses on photovoltaic (PV) solar cells.

More in details, the work deals on the analysis of parameters extraction techniques for the modelling of kesterite and crystalline silicon (c-Si) solar cells. The aim of the study is to perform the simulation of the electronic circuit of a tandem-configuration of solar cells having the kesterite cell on the top and the c-Si as the bottom one. Results obtained in the simulations of the tandem configurations can help to predict the maximum values of expected efficiency and also to improve the fabrication process of the kesterite top cell in order to obtain the most efficient tandem configuration.

So, both the kesterite and the c-Si solar cells have been modelled using the five parameter model which emerged as the most suitable one to be applied for this work’s objectives. Simulations have been performed in two different environment, Matlab and PSpice, and the results obtained from the modelling procedure have been validated by comparison with the measured data. Moreover, EQE measurements of both cell technologies have been analysed in order to complete the cells’ characterization and to observe the useful spectrum range in terms of photon absorption.

Then, the electric tandem simulation has been performed, using PSpice again, and it has been observed how the efficiency changed with the variation of the bottom cell current density. Results show that good efficiency can be reached. In particular, a value of 22.5% is achievable with a reasonable current density of 32 mA/cm^2. Anyway, to do that, the optical properties of the top kesterite-based solar cell have to be improved in order to allow higher transmission, above all at high longwave. It can be done reducing its reflectivity and increasing the band-gap of the absorber layer.

Abstract

Negli ultimi anni si è parlato spesso di “transizione energetica”. Con essa si intende l’interesse crescente della gente coinvolta nel settore della produzione di energia verso le sorgenti energetiche non convenzionali con le quali si cercherà di soddisfare i fabbisogni energetici della società, in sostituzione delle fonti fossili convenzionali. Anche governi nazionali ed organizzazioni internazionali (ad esempio l’Unione Europea) stanno sviluppando dei programmi e fissando degli obiettivi col fine di accelerare questa transizione energetica. Queste sono alcune delle ragioni per cui le tecnologie energetiche rinnovabili stanno vivendo una crescita così rapida. Tra le varie alternative, questo lavoro è focalizzato sulle celle fotovoltaiche.

In particolare, vengono trattate tecniche di estrazione dei parametri, usate per la modellizzazione di celle fotovoltaiche di kesterite e di silicio cristallino. Lo scopo dello studio è quello di realizzare la simulazione del circuito elettronico di una configurazione tandem di queste due celle, avente la cella di kesterite posizionata sopra quella di silicio cristallino. I risultati che verranno ottenuti nelle simulazioni delle configurazioni tandem possono aiutare a prevedere le massime efficienze raggiungibili ed a migliore il processo di fabbricazione delle celle a base di kesterite in modo da ottenere la configurazione tandem più efficiente possibile.

Quindi, entrambe le tecnologie di cella fotovoltaica sono state modellizzate usando il modello dei cinque parametri, il quale è emerso come il più adeguato per essere utilizzato ai fini di questo lavoro. Le simulazioni sono state effettuate usando due diversi ambienti informatici, Matlab e PSpice, e i risultati così ottenuti dalla modellizzazione son stati convalidati tramite un confronto con i dati provenienti dalle reali misurazioni sulle prestazioni delle celle. Inoltre, per completare la caratterizzazione, son stati analizzati anche dati sull’efficienza quantica esterna (EQE), utili anche per avere un’idea sul comportamento spettrale in termini di assorbimento fotonico.

Successivamente è stata effettuata la simulazione del tandem, utilizzando PSpice, ed è stato osservato come varia l’efficienza al variare della densità di corrente della cella inferiore (c-Si). I risultati mostrano che può essere raggiunta una buona efficienza. In particolare, è raggiungibile un valore del 22.5% con una densità di corrente di 32 mA/cm^2. Comunque, per

far ciò, devono essere migliorate le proprietà ottiche della cella di kesterite, per permettere un'elevata trasmittanza, soprattutto ad elevate lunghezze d'onda. Ciò può essere fatto riducendo la riflessività ed aumentando il band-gap dello strato assorbitore.

Table of Contents

List of Figures

List of Tables

1. Introduction

1.1 – Overview

In the last decades, a lot of attention has been given to the renewable energy technologies. In particular, it happened due to the growing interest in environmental issues, the awareness that fossil fuel resources are not unlimited, and also in order to guarantee more security in terms of energy supply to those Countries which have not so much fossil fuel resources and that are dependent from abroad importation.

The International Energy Outlook (IEO) 2017 has reported an increasing world energy consumption from 1990 to 2015 [1]. Moreover, projections have shown that consumption will rise by 28% from 2015 to 2040, with more than half of the increase attributed to non-OECD (Organization for Economic Cooperation and Development) Asia (Fig. 1), where Nations like India and China are living a huge economic growth requiring high demand for energy.

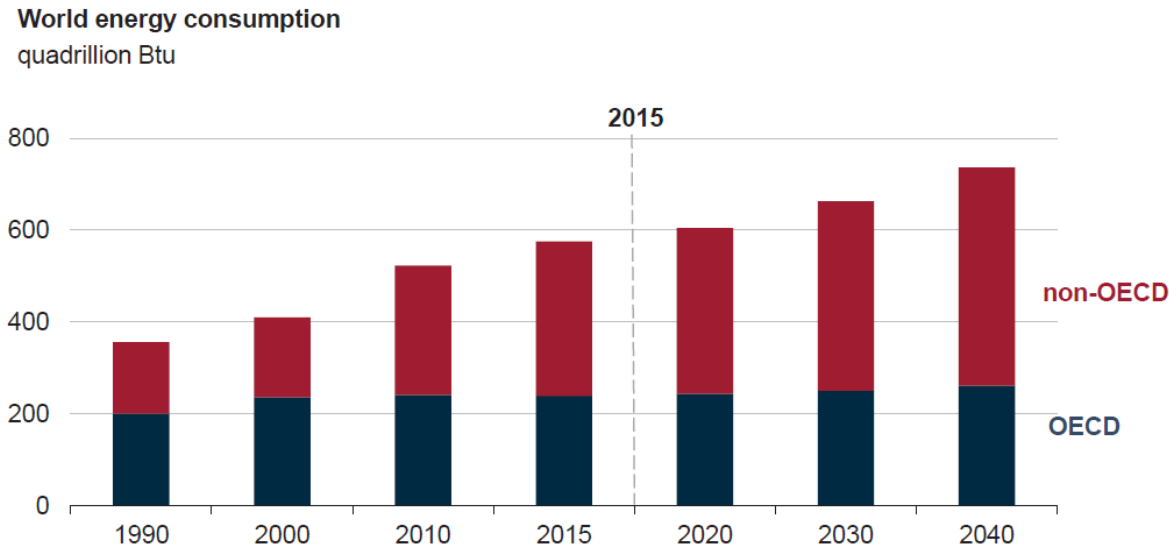

Figure 1: *World energy consumption evolution [1].*

Effectively, energy is defined as the "availability to do work", so an easy access to energy is the key point for the development of a society. One more proof to this theory comes from the relation between Gross Domestic Product and electricity consumption. In fact, it has

been pointed out that, globally, an increasing in the GDP is followed by a higher electricity consumption [2]. This relationship between the two magnitudes occurs also during crisis time, but in the opposite way (Fig.2).

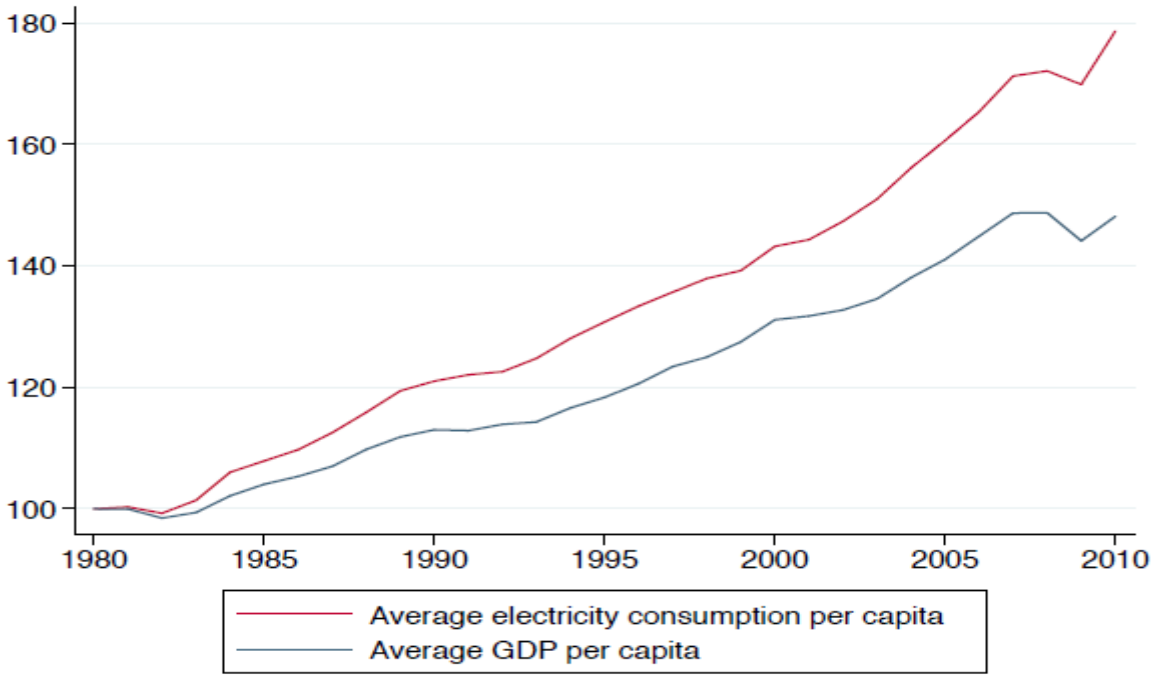

***Figure 2**: Evolutions of electricity consumption and GDP for 160 countries [2].*

The meaning of all these information is that there could not be progress without energy. Focusing just on the electricity production, nowadays, its generation occurs mainly by fossil fuel, with coal as the main player, followed by natural gas.

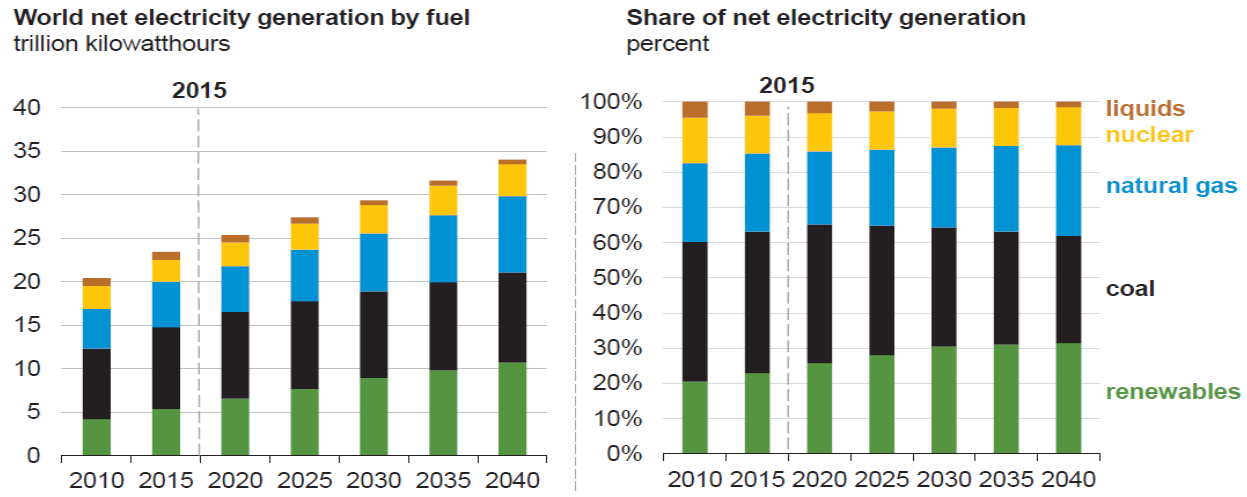

***Figure 3**: Electricity market share per technology [1].*

However, it is expected a big increase of renewables in the market share, making them the fastest-growing sources of electricity generation for the period 2015-2040 (Fig.3).

Among the several renewable energy technologies, this work is focused on solar photovoltaics. By mean of little devices, as a solar cell is, this technology allows to convert the photon's radiative energy from the Sun into electrical power.

Briefly, the solar cells were first used in space application as an alternative to batteries, since they offered a higher power-to-weight ratio. However the growing interest has soon focused in energy application. It could be possible thanks to the relevant cost reduction suffered by these devices, and the huge effort in research and development. In particular, attention has been given to the materials, according their several properties. In fact, a solar cell must be composed by semiconductor materials, even suffering a doping phase, in order to create a p-n junction allowing the electrons moving in the structure and creating a circulating current.

Solar photovoltaic cells have seen a huge development along the years, and in fact they are grouped according three different generations. In any case, different substances can be used to build up the absorber layer of a solar cell. Traditionally, silicon has been used, but new materials are emerging. Among them, there is the Kesterite, which is a sulphide mineral belonging to the chalcogenide family. Anyway, different technologies have different level of maturity and it affects a lot the performances of each one.

1.2 – State of the art

As written before, today, solar cells are classified into three generations. The first generation cells, the wafer based ones, are made of crystalline silicon and today they are the predominant PV technology in the market (Fig. 4). Second generation cells include the so called "thin film" solar cells and they are made up by amorphous silicon, CdTe or CIGS. Their share in the market is increasing but it still is much lower than the c-Si solar cells.

Finally the third generation. It includes a lot of cells technologies, in particular thin-film technology again, but most of them are still in research phase and they did not suffer commercial application.

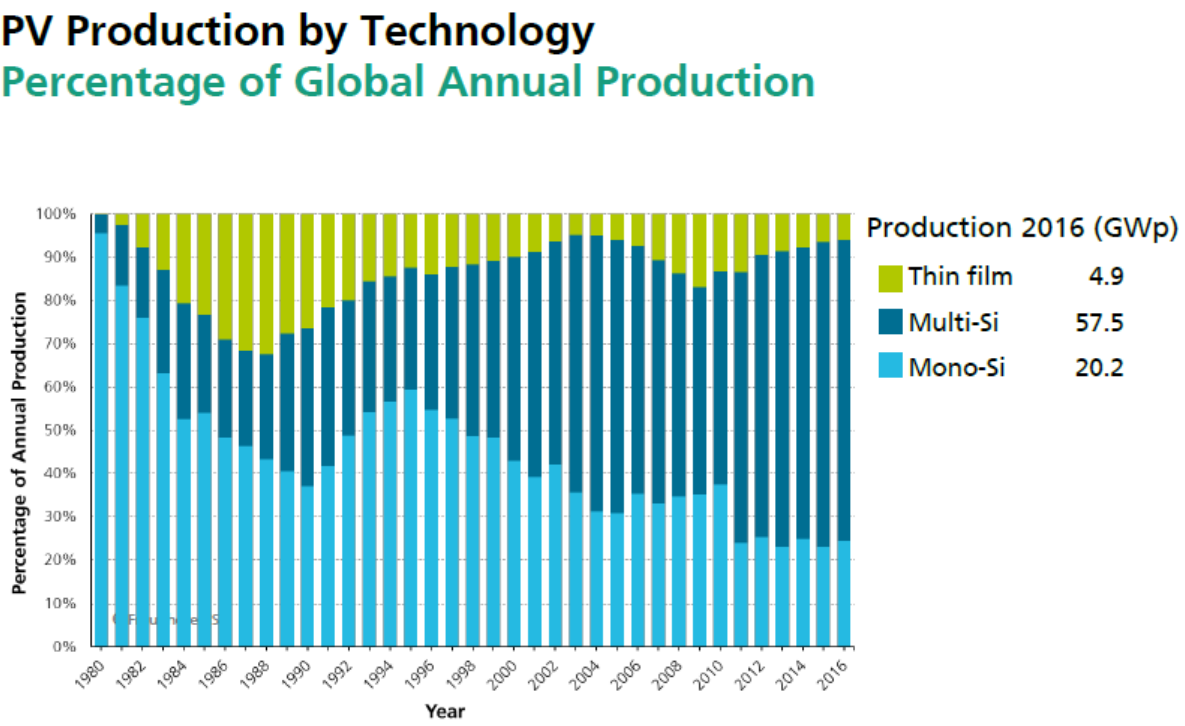

***Figure 4**: PV production by technology [3].*

In all these cases we are considering that the device is composed by one single layer of light-absorbing material. However solar cells can be also made up using multiple physical configurations trying to enhance the sunlight absorption. They are the so called multi-junctions.

This work aims to analyse a particular kind of multi-junction solar cell, such as a tandem configuration. A tandem configuration consists of two different solar cells, possibly characterized by different properties, in particular the energy band-gap, arranged one over the other and usually in a series connection. The goal is to improve the efficiency achievable by one single cell.

To do that, specific materials have to be chosen. This study focuses on kesterite and crystalline silicon, which have very different history in the photovoltaic field.

In fact, c-Si based solar cell is the most mature technology. Since the beginning of the first applications, silicon showed good properties, making it a suitable material for photovoltaics. So, year by year the technology has being improved, and it follows that, for single-junction cells, the highest recorded efficiencies belong to this family of cells. In particular, in 2017, the best mono crystalline silicon solar cell performed an efficiency of almost 26.7%, while for multi-crystalline it reaches almost 21.9% [4] (Table 1).

On the other hand, researchers were looking for alternatives to silicon and several materials had tested all over the years. Among them, there are Gallium, Arsenic, Indium, the whole family of chalcogenide materials and so on. However, there are several reasons why interest in kesterite based solar cells (CZTS, CZTSE, CZTSSe) is growing so much during last years.

In fact, even if thin film chalcopyrite photovoltaics based on CIGS and relative alloys are already playing an active role in the market and they also achieved a good record efficiency at laboratory scale of 21.7% [4], their production is expected to be limited. This is due to the scarcity of element such as Indium and Gallium, also causing a high production cost.

At the meantime other technologies, such as CdTe solar cells are suffering problems related to the Cadmium toxicity.

On the other hand, in kesterite compounds the scares element of CIGS are substituted by the abundant zinc and tin, and the toxicity problems related to Cd use are avoided.

Moreover, such compounds have demonstrated high absorption coefficient in the range of 10^4 cm^{-1} and a direct band gap between 1 and 1.5 eV, allowing an effectively huge photon absorption with very low absorber thickness [5].

For these reasons, it seems that kesterite compounds could be promising materials for upcoming application in solar cells.

Moreover, it is clear that a lot of other requirements have to be meet, in particular in terms of specific physical properties.

In fact, for PV application, a good material should also guarantee favourable transport properties, suitable band edge position and of course high carrier lifetime.

Anyway, some experiments had already performed, and at the current state of the art, the record efficiency for a CZTSSe solar cell reached a value of 12.6%, in 2013 [6]. A much higher value, almost 18%, is needed to allow this technology to enter the market, and kesterite based solar cells to be produced at commercial level, but for sure it is a good starting point.

The following Table 1 and Table 2 show the efficiencies reached by the several solar cell technologies until 2017.

Classification	Efficiency (%)	Area (cm^2)	V_{oc} (V)	J_{sc} (mA/cm^2)	Fill Factor (%)	Test Centre (date)	Description
Silicon							
Si (crystalline cell)	**26.7 ± 0.5**	**79.0 (da)**	**0.738**	**42.65[a]**	**84.9**	**AIST (3/17)**	**Kaneka, n-type rear IBC[5]**
Si (multicrystalline cell)	**21.9 ± 0.4[b]**	**4.0003 (t)**	**0.6726**	**40.76[a]**	**79.7**	**FhG-ISE (2/17)**	**FhG-ISE, n-type[6]**
Si (thin transfer submodule)	21.2 ± 0.4	239.7 (ap)	0.687[c]	38.50[c,d]	80.3	NREL (4/14)	Solexel (35 µm thick)[7]
Si (thin film minimodule)	10.5 ± 0.3	94.0 (ap)	0.492[c]	29.7[c]	72.1	FhG-ISE (8/07)[e]	CSG Solar (<2 µm on glass)[8]
III-V cells							
GaAs (thin film cell)	28.8 ± 0.9	0.9927 (ap)	1.122	29.68[f]	86.5	NREL (5/12)	Alta Devices[9]
GaAs (multicrystalline)	18.4 ± 0.5	4.011 (t)	0.994	23.2	79.7	NREL (11/95)	RTI, Ge substrate[10]
InP (crystalline cell)	**24.2 ± 0.5[b]**	**1.008 (ap)**	**0.939**	**31.15[a]**	**82.6**	**NREL (9/12)**	**NREL[11]**
Thin film chalcogenide							
CIGS (cell)	**21.7 ± 0.5**	**1.044 (da)**	**0.718**	**40.70[a]**	**74.3**	**AIST (1/17)**	**Solar Frontier[12]**
CdTe (cell)	21.0 ± 0.4	1.0623 (ap)	0.8759	30.25[d]	79.4	Newport (8/14)	First Solar, on glass[13]
CZTS (cell)	**10.0 ± 0.2**	**1.113 (da)**	**0.7083**	**21.77[a]**	**65.1**	**NREL (3/17)**	**UNSW[14]**
Amorphous/microcrystalline							
Si (amorphous cell)	10.2 ± 0.3[g,b]	1.001 (da)	0.896	16.36[d]	69.8	AIST (7/14)	AIST[15]
Si (microcrystalline cell)	**11.9 ± 0.3[b]**	**1.044 (da)**	**0.550**	**28.72[a]**	**75.0**	**AIST (2/17)**	**AIST[16]**
Perovskite							
Perovskite (cell)	19.7 ± 0.6[g,h]	0.9917 (da)	1.104	24.67[i]	72.3	Newport (3/16)	KRICT/UNIST[17]
Perovskite (minimodule)	**16.0 ± 0.4[g,h]**	**16.29 (ap)**	**1.029[c]**	**19.51[c,a]**	**76.1**	**Newport (4/17)**	**Microquanta, 6 serial cells[18]**
Dye sensitised							
Dye (cell)	11.9 ± 0.4[j]	1.005 (da)	0.744	22.47[k]	71.2	AIST (9/12)	Sharp[19]
Dye (minimodule)	10.7 ± 0.4[j]	26.55 (da)	0.754[c]	20.19[c,l]	69.9	AIST (2/15)	Sharp, 7 serial cells[19]
Dye (submodule)	8.8 ± 0.3[j]	398.8 (da)	0.697[c]	18.42[c,m]	68.7	AIST (9/12)	Sharp, 26 serial cells[20]
Organic							
Organic (cell)	11.2 ± 0.3[n]	0.992 (da)	0.780	19.30[d]	74.2	AIST (10/15)	Toshiba[21]
Organic (minimodule)	9.7 ± 0.3[n]	26.14 (da)	0.806	16.47[c,l]	73.2	AIST (2/15)	Toshiba (8 series cells)[22]

Abbreviations: CIGS, $CuIn_{1-y}Ga_ySe_2$; a-Si, amorphous silicon/hydrogen alloy; nc-Si, nanocrystalline or microcrystalline silicon; CZTSS, $Cu_2ZnSnS_{4-y}Se_y$; CZTS, Cu_2ZnSnS_4; (ap), aperture area; (t), total area; (da), designated illumination area; FhG-ISE, Fraunhofer Institut für Solare Energiesysteme; AIST, Japanese National Institute of Advanced Industrial Science and Technology.

Table 1: Solar cells efficiency at STC by cell technology until 2017 [4].

Classification	Efficiency (%)	Area (cm^2)	V_{oc} (V)	J_{sc} (mA/cm^2)	Fill Factor (%)	Test Centre (date)	Description
Cells (silicon)							
Si (crystalline)	25.0 ± 0.5	4.00 (da)	0.706	42.7[a]	82.8	Sandia (3/99)[b]	UNSW p-type PERC top/rear contacts[40]
Si (crystalline)	**25.7 ± 0.5[c]**	**4.017 (da)**	**0.7249**	**42.54[d]**	**83.3**	**FhG-ISE (3/17)**	**FhG-ISE, n-type top/rear contacts[41]**
Si (large)	**26.6 ± 0.5**	**179.74 (da)**	**0.7403**	**42.5[d]**	**84.7**	**FhG-ISE (11/16)**	**Kaneka, n-type rear IBC[5]**
Si (multicrystalline)	21.3 ± 0.4	242.74 (t)	0.6678	39.80[e]	80.0	FhG-ISE (11/15)	Trina Solar, large p-type[42]
Cells (III-V)							
GaInP	21.4 ± 0.3	0.2504 (ap)	1.4932	16.31[f]	87.7	NREL (9/16)	LG Electronics, high bandgap[43]
Cells (chalcogenide)							
CIGS (thin-film)	22.6 ± 0.5	0.4092 (da)	0.7411	37.76[f]	80.6	FhG-ISE (2/16)	ZSW on glass[44]
CIGSS (Cd free)	**22.0 ± 0.5**	**0.512 (da)**	**0.7170**	**39.45[f]**	**77.9**	**FhG-ISE (2/16)**	**Solar Frontier on glass[12]**
CdTe (thin-film)	22.1 ± 0.5	0.4798 (da)	0.8872	31.69[g]	78.5	Newport (11/15)	First Solar on glass[45]
CZTSS (thin-film)	12.6 ± 0.3	0.4209 (ap)	0.5134	35.21[h]	69.8	Newport (7/13)	IBM solution grown[46]
CZTS (thin-film)	**11.0 ± 0.2**	**0.2339(da)**	**0.7306**	**21.74[d]**	**69.3**	**NREL (3/17)**	**UNSW on glass[14]**
Cells (other)							
Perovskite (thin-film)	22.1 ± 0.7[i]	**0.0946 (ap)**	1.105	24.97[j]	80.3	Newport (3/16)	KRICT/UNIST[17]
Organic (thin-film)	**12.1 ± 0.3[k]**	**0.0407 (ap)**	**0.8150**	**20.27[d]**	**73.5**	**Newport (2/17)**	**Phillips 66**

Abbreviations: CIGSS, CuInGaSSe; CZTSS, $Cu_2ZnSnS_{4-y}Se_y$; CZTS, Cu_2ZnSnS_4; (ap), aperture area; (t), total area; (da), designated illumination area; AIST, Japanese National Institute of Advanced Industrial Science and Technology; NREL, National Renewable Energy Laboratory; FhG-ISE, Fraunhofer-Institut für Solare Energiesysteme.

Table 2: Notable exceptions: Top dozen confirmed cell and module results at STC until 2017 [4].

2. Modelling and simulation of I-V characteristics.

2.1 - Kesterite solar cell

Kesterite is a sulphide mineral composed by copper, zinc, tin, sulphur, and little quantity of iron. It can also be produced synthetically and such a form of kesterite is abbreviated as CZTS (copper zinc tin sulphide). However, some synthetic materials contain selenium instead of sulphur (CZTSe) and they are also referred as kesterite. Interest in such a substance is growing really fast and a lot of effort is being putted in research for use in solar photovoltaic application. There are several reasons behind this choice. In fact, even if silicon solar cells are still dominant in the market [3], some alternative materials have been using to produce solar cells. In particular, they are chalcopyrite compounds based on CIGS (copper indium gallium selenide) and cadmium telluride (CdTe). However, as already introduced, indium and gallium are suffering scarcity issues, while cadmium has some problems due to toxicity. It follows that kesterite appears like a promising alternative, since its elements are all abundant and the electronic properties seem to be suitable for photovoltaic application. The energy bandgap of these semiconductors materials, in fact, is between 1 and 1.5 eV, depending by the percentage of the different elements and, above all, by the sulphur over selenium ratio [6]. A value inside this range should allow a huge photon absorption that is what researchers look for.

2.1.1 - Fabrication process

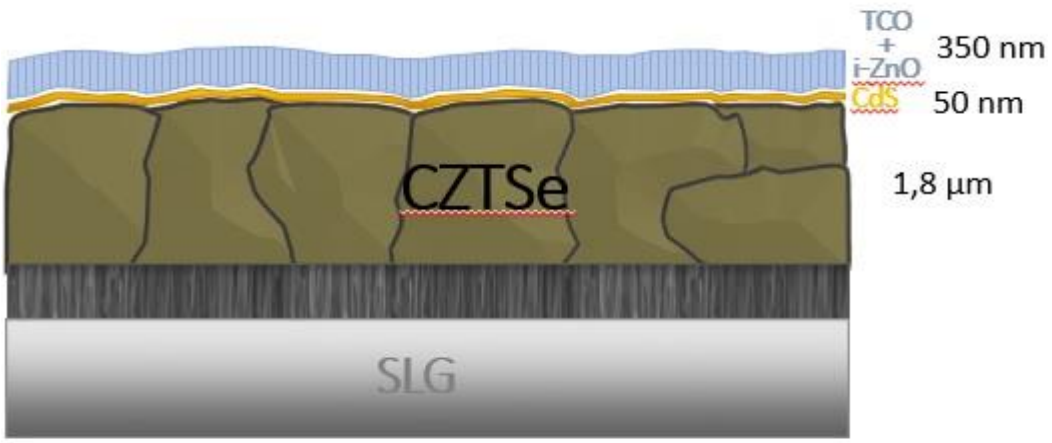

***Figure 5**: Kesterite based solar cell's structure [7].*

The kesterite based solar cell used in this study has the following structure (Fig. 5). From bottom to top: the first layer is a Soda-Lime Glass (SLG). It plays mainly a support function and its thickness is in the range of 2 and 3 mm.

Then, there is the back contact. The chosen metal is Molybdenum, because its properties allow getting a suitable value of the metal work function, allowing to get the best from the cell performances.

The thickness of that layer is between 750 and 800 nm.

Later, there is a precursor layer of Cu/Sn/Cu/Zn, with a thickness of 500 nm. It just precedes the Kesterite absorber layer, probably the most interesting one, at least for this study. This layer should guarantees certain features in order to provide suitable properties, in particular in terms of charge carriers transport, band edge position and carrier lifetime. Not considering the SLG layer, it is the thicker one (1.8 micron).

Continuing towards the top, there is the CdS buffer layer. Its role is to improve the interface properties and to protect the absorber layer. In that cell, it has a thickness of 50 nm.

At the end there are the zinc oxide layer (ZnO) and the transparent indium tin oxide layer. The total thickness is around 350 nm.

To build the whole assembly, some steps are needed [7].

First of all, attention is put over the synthesis of CZTSe, which is performed by a sequential process. So, SLG/Mo/Cu/Sn/Cu/Zn metallic precursor stacks were deposited by DC-magnetron sputtering onto Mo coated soda-lime glass substrates. The films have a chemical composition near the range of those reported as ideal for high efficiency solar cells that means Cu-poor and Zn-rich.

Precursors were then selenized by rapid thermal processes (RTP) using an AnnealSys AS-ONE-100 furnace in a semi-closed system made up by a graphite box with a reaction volume of 3.8 cm^3. During this step, approximately 20 mg elemental Se (Alfa Aesar, 99.999% purity) were placed into the box next to the substrates. The reactive annealing was performed in a two-step process: (1) heating from room temperature to 400 °C with a ramp of 180 °C/min and (2) heating to 500 °C with a ramp of 60 °C/min. After the second step, the sample was cooled to below 80 °C.

At this point, the characterization of precursor stacks and annealed CZTSe films occurs. It was performed by X-ray fluorescence (XRF), and the aim is to determine the exact

compositions. In addition, a phase analysis was performed by combining X-ray diffraction (XRD) and Raman spectroscopy (RS).

Now, the kesterite absorbers were synthesized and characterized, and solar cell devices are ready to be fabricated with selected samples. First, in order to remove the possible presence of secondary phases (mainly ZnSe and SnSe), the films were etched in H_2SO_4 + $KMnO_4$ and $(NH_4)_2S$ solutions. Next, the CdS buffer layer was deposited via chemical bath deposition (CBD). Then, i-ZnO and ITO layers were deposited by pulsed DC-magnetron sputtering and finally the cells were mechanically scribed to complete the device fabrication.

2.1.2 - Real I-V's measurements and cell characterization

The real I-V measurements are the starting point for the modelling and simulation of this thesis work. In fact they allow characterizing the analysed solar cells and also to compare the results will be obtained by simulation.

The data have been provided by IREC, the Energy Research Institute of Catalonia.

More in details, several solar cells performances have been measured, both in light (STC) and dark conditions. The data corresponding to measurements carried out in light conditions, are particularly relevant for the characterization of the solar cells, so to evaluate their performance. However, combining light and dark measurements data it has been possible to model the several cells, finding the model's parameters needed to describe the behaviour.

So, inside a voltage range limited by an upper and a lower value, for each voltage value the corresponding current has been measured and provided. It has been done in both condition. However, the voltage range is not the same for all the cells. It depends by several factors. In particular, the different cells have different dimension and this fact affects the output. Consequently, the interesting voltage range will change and so the upper and limit values taken in the measurements. Of course also the intrinsic characteristics of the cells will affect the behaviour and, as a consequence, it has been taken into account during the measurements.

So, from the light measurements some important parameters can be extracted: the open circuit voltage, the short circuit current, the fill factor and the solar cell efficiency.

Very briefly, the open circuit voltage (V_{OC}) is the voltage difference between the two terminals of the solar cell when no external load is applied, so when it is disconnected from any circuit.

The short circuit current (I_{SC}) instead, is the current would flow in the device if no voltage drop occurred in the solar cell, that means the load voltage is null and the related resistance almost zero. In this case the I_{SC}, so the cell current, is equal to the photo-generated one, and it is the maximum current the cell can provide.

Then, the fill factor (FF) is a parameter showing the quality of the solar cell, since it gives an idea about how much the cell behaviour is close to the ideal one. It is the ratio between the maximum power point voltage (V_m) multiplied by the maximum power point current (I_m), and the open circuit voltage multiplied by the short circuit current, according to equation 1.

$$FF = \frac{V_m I_m}{V_{oc} I_{sc}} \quad (1)$$

Obviously, it is always lower than one, but the closer the value of the FF is to the unity, the better the operation of the solar cell.

Finally, the efficiency: probably it is the most significant parameter since it gives the measure of how much power can be extracted from a given resource. So higher the efficiency, better the resource utilization. In the case of PV solar cells it is defined by the equation 2:

$$\eta = \frac{I_m V_m}{G_{STC} A} \quad (2)$$

Where "A" is the solar cell area, "G_{STC}" is the standard irradiance, conventionally equal to 1000 W/m^2, spectrum AM 1.5.

"I_m" and "V_m" are the same values used in the equation 1. Just as a reminder, they are respectively, the current measured at the point in which the cell provide the maximum power and the voltage measured at the same point.

So, in this study, ten different solar cells were analysed. The results are summarized in the table 3.

Solar cell	1	2	3	4	5	6	7	8	9	10
Isc(mA)	16.0	15.6	17.9	15.7	14.9	14.5	15.2	19.7	22.7	17.4
Voc(mV)	412.0	407.7	413.4	409.0	321.1	349.2	357.9	382.9	387.6	381.2
Im(mA)	12.8	12.7	14.3	12.7	10.8	10.3	11.4	14.6	16.8	12.8
Vm(mV)	282.7	294.0	293.8	293.8	203.3	237.7	237.3	260.0	260.0	260.0
η(%)	6.70	7.04	6.46	6.66	4.00	4.53	4.83	5.66	5.67	5.64
FF	0.548	0.587	0.569	0.582	0.459	0.483	0.496	0.502	0.497	0.503
Area(cm^2)	0.54	0.53	0.65	0.56	0.55	0.54	0.56	0.67	0.77	0.59

Table 3: Kesterite based solar cells' characterization.

2.1.3 - Parameters extraction

The parameter extraction is one other key point of the study. The aim is to find the parameters which characterize the solar cell, and its model, and that affect its behaviour in terms of I-V curve and performance. It has been decided to use the one diode model, also known as five parameters model [9].

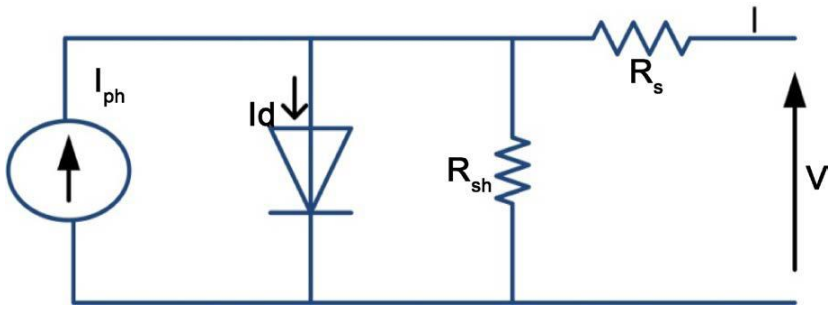

***Figure 6**: Five parameters model circuit [9].*

The governing equation is the following one (3):

$$I_{cell} = I_{ph} - I_0\left[e^{\frac{V_{cell}+I_{cell}R_S}{nV_T}} - 1\right] - \frac{V_{cell}+I_{cell}R_S}{R_p} \quad (3)$$

The several factors are:

- I_{cell}: the output current;
- V_{cell}: the output voltage;
- I_{ph}: the photo-generated current;
- I_0: the diode reverse saturation current;

- n: the diode ideality factor;
- V_T: the thermal voltage;
- R_s: the series resistance;
- R_p: the shunt resistance.

The thermal voltage is calculated as: $V_T = \frac{kT}{q}$.

Where "k" is Boltzmann's constant, "T" the absolute temperature and "q" the elementary charge.

The model is so called because it is based on five parameters, which characterize the solar cell and determine its behaviour.

They are: the short circuit current density, "J_{sc}", the series resistance, "R_s", the shunt resistance, "R_p", the ideality factor, "n", and the saturation current, "I_0".

Considering that the photo-generated current is strictly related to Jsc, it can be observed that all the parameters are involved in the model equation (3).

Through this equation, the relation between voltage and current can be found and, as a consequence, the I-V curve of the solar cell can be obtained.

However, all the others parameters have to be known.

To get them, during the parameters extraction procedure, a Matlab code was used, based on the Newton-Raphson algorithm.

So, starting from a set of parameters, the code evaluated a fictitious parameter defined as the difference between two consecutive evaluations of the investigated quantity. When the value of the fictitious parameter is small enough, the computed value of our unknown is saved. It is repeated several times, depending by the voltage vector length in input, and as a result the I-V curve is shown. If the results were not good, one or more than one parameter were changed, in order to get a better fitting with respect to the real data. The variation of the parameter is based on the theoretical knowledge.

This procedure were developed for both light STC and dark condition measurements. What was expected was that for each solar cell, the parameters had the same values in both conditions. However, during the extraction process, it has been pointed out that the series resistance suffered a small variation between the light and dark simulation. This phenomenon has been taken into account, but it is not considered as anomalous because there are several examples in literature where this phenomenon has been reported and

analysed [10]. The conclusion is that, at micro-scale analysis, the cell structure suffers little variation depending by the photon radiation and it affects its properties, in particular the series resistance.

After that, once the results are suitable, the five parameters are saved and the simulated results are compared with the real ones and eventually validated.

Now, for each solar cell, the five parameter will be summarized in table 4 and table 5.

Solar cell	1	2	3	4	5	6	7	8	9	10
Jsc(A/cm^2)	0.030	0.029	0.028	0.028	0.027	0.027	0.027	0.029	0.029	0.029
Rs(Ohm)	1.4	1.1	1.5	1.5	2.5	2	2	1.9	1.7	1.7
Rp(Ohm)	300	500	500	500	200	150	180	170	150	150
n	1.83	1.974	2	2	1.76	2	2	1.73	1.75	1.83
I_0(A)	$2\ 10^{-6}$	$5\ 10^{-6}$	$5\ 10^{-6}$	$5\ 10^{-6}$	$1\ 10^{-5}$	$1\ 10^{-5}$	$1\ 10^{-5}$	$3\ 10^{-6}$	$3.9\ 10^{-6}$	$4\ 10^{-6}$

Table 4: Five parameters in STC.

Solar cell	1	2	3	4	5	6	7	8	9	10
Jsc(A/cm^2)	0.030	0.029	0.028	0.028	0.027	0.027	0.027	0.029	0.029	0.029
Rs(Ohm)	4	1.15	1.2	1.8	8	4	3	2	1.8	2.2
Rp(Ohm)	300	500	500	500	200	150	180	170	200	150
n	1.83	1.974	1.75	2	1.76	2	2	1.73	1.75	1.83
I_0(A)	$2\ 10^{-6}$	$5.5\ 10^{-6}$	$6\ 10^{-6}$	$5\ 10^{-6}$	$1\ 10^{-5}$	$1.3\ 10^{-5}$	$1.2\ 10^{-5}$	$3\ 10^{-6}$	$3.9\ 10^{-6}$	$4\ 10^{-6}$

Table 5: Five parameters in dark condition.

2.1.4 - Validation and comparison between real and simulated data

When the simulation is concluded, the results are compared with the real measured ones. The comparison was made in terms of I-V curve, because it is the most important tool by which the behaviour of the solar cell can be checked point by point inside the desired voltage range. To ensure that the solar cell has been well characterized, the comparison has been made both in light STC and in dark conditions.

The parameter used as a quality factor was the Root Mean Square Error (RMSE). It is defined by the following equation (4):

$$RMSE = \sqrt{\frac{\sum_{t=1}^{n}(y_m - y_s)^2}{n}} \quad (4)$$

Where:

- y_m is the measured value;
- y_s is the simulated value;
- n is the number of point.

Obviously, the compared quantity is the current, since the voltage is defined as an input and it is set equal to the measured values.

So, if the RMSE is lower than a minimum value (1[mA]), the simulation is considered good and the results validated. Of course, for the same solar cell, it must happen for both the light and dark simulation.

Therefore, among the several cells simulated, suitable results have been obtained in ten cases, corresponding to the same solar cells listed in the tables 3, 4 and 5.

The accuracy of the results, anyway, is different case by case. In fact, even if the RMSE constraint has been always satisfied, in some cases the fitting is not so good as it was hoped. In particular, in those cases it has been seen that the deviation of the simulated results from the measured ones was still significant in that zone around the maximum power point for some cells or at very high voltage for others.

It is reasonable to think that the reason is not strictly related to the values of the chosen parameters, but in the model used for the simulation. So, to improve the simulation, it could be tried using a more accurate one (e.g. the two diodes model [9]), but probably the gain wouldn't be so huge to justify it.

On the other hand, instead, for certain cells really accurate results have been simulated allowing to get a really small RMSE, proving the validity of the model.

In any case, all these peculiarity can be now analysed more in detail, showing the obtained results.

2.1.4.1 – Cell 1

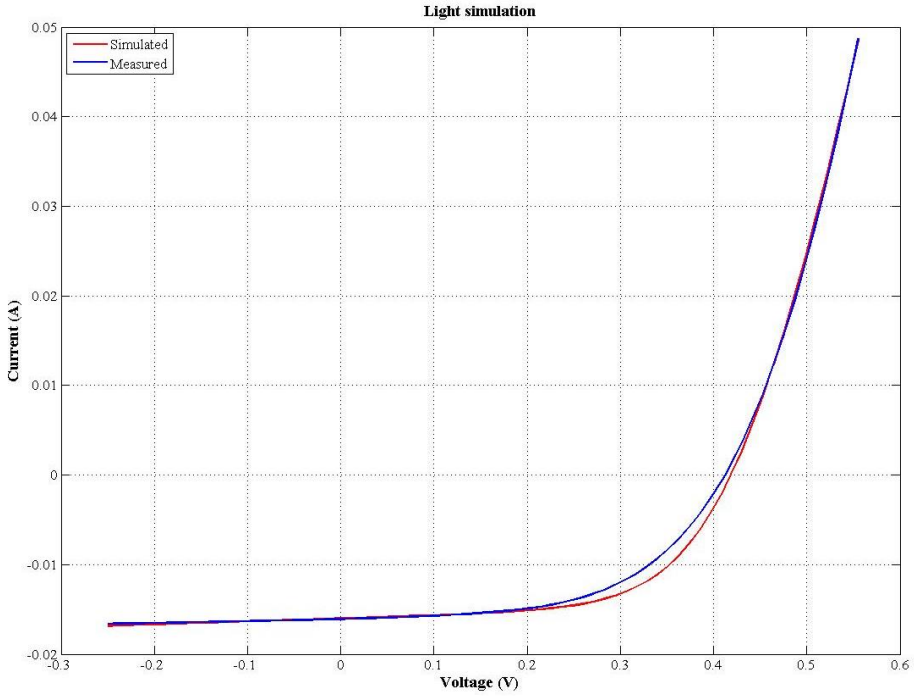

***Figure 7**: Light simulation of cell 1.*

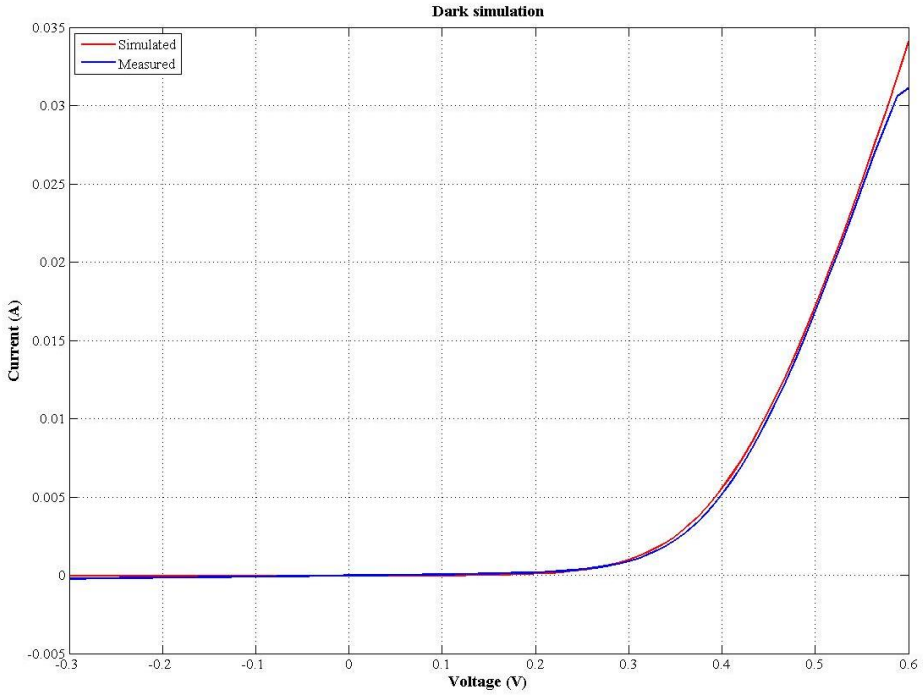

***Figure 8**: Dark simulation of cell 1.*

Cell 1	Light	Dark
RMSE (mA)	0.728	0.43
RMSE (%)	4.5	2.6

Table 6: RMSE of cell 1 simulation.

2.1.4.2 – Cell 2

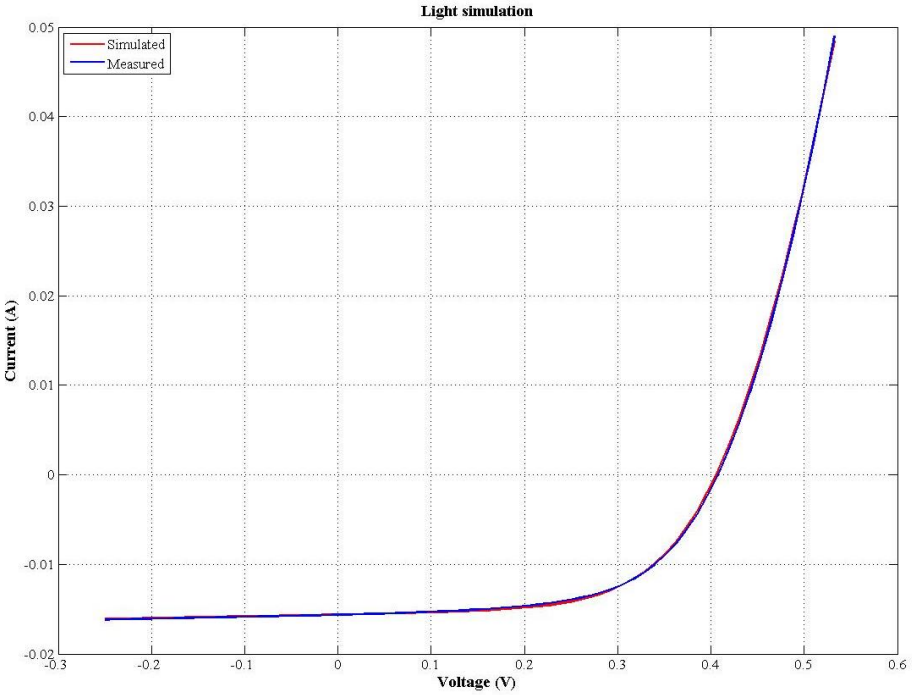

***Figure 9**: Light simulation of cell 2.*

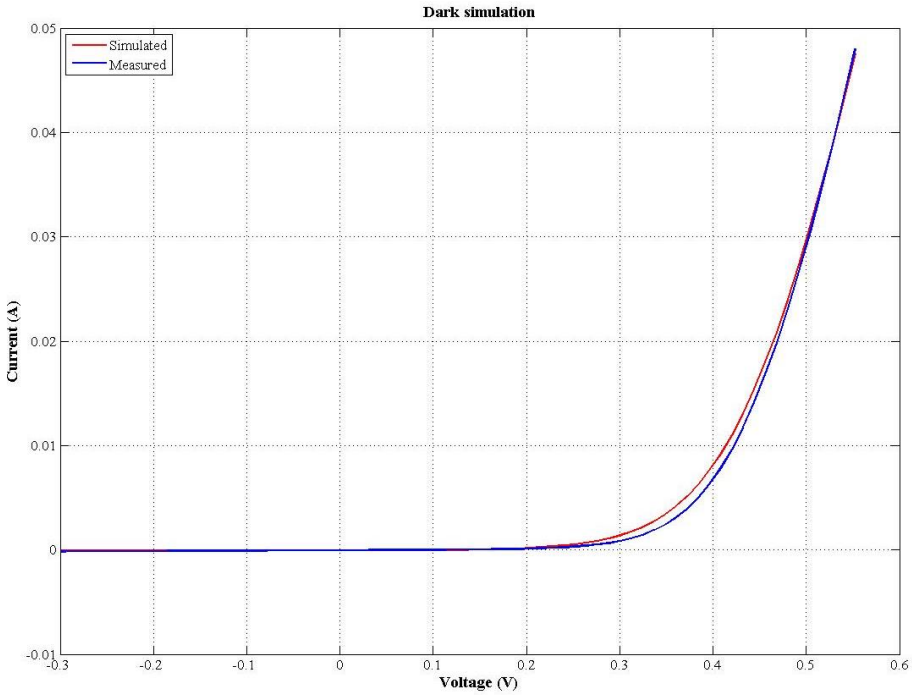

***Figure 10**: Dark simulation of cell 2.*

Cell 2	Light	Dark
RMSE (mA)	0.233	0.53
RMSE (%)	1.5	3.4

Table 7: RMSE of cell 2 simulation.

2.1.4.3 – Cell 3

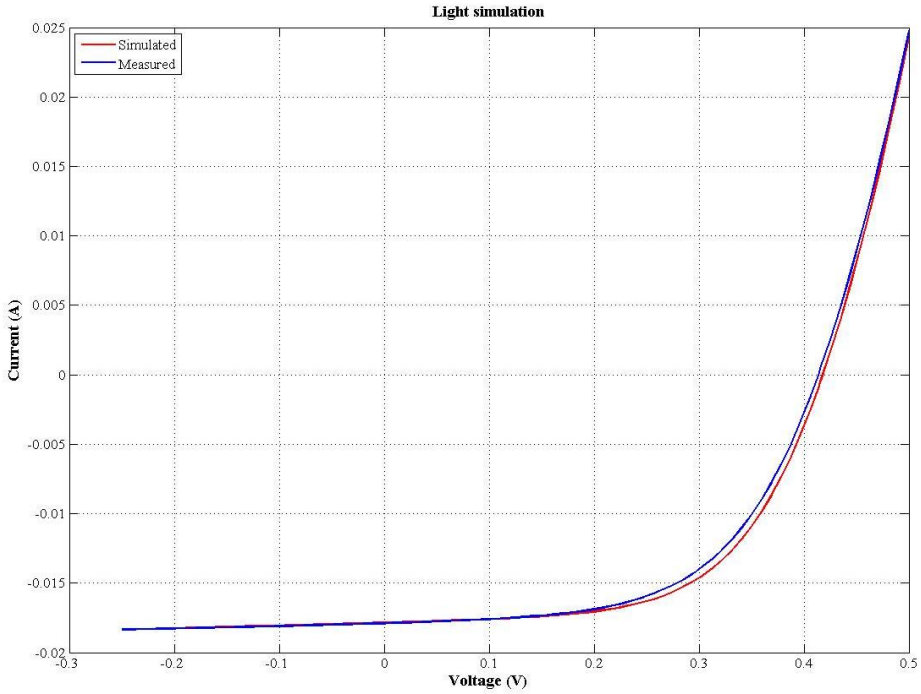

***Figure 11**: Light simulation of cell 3.*

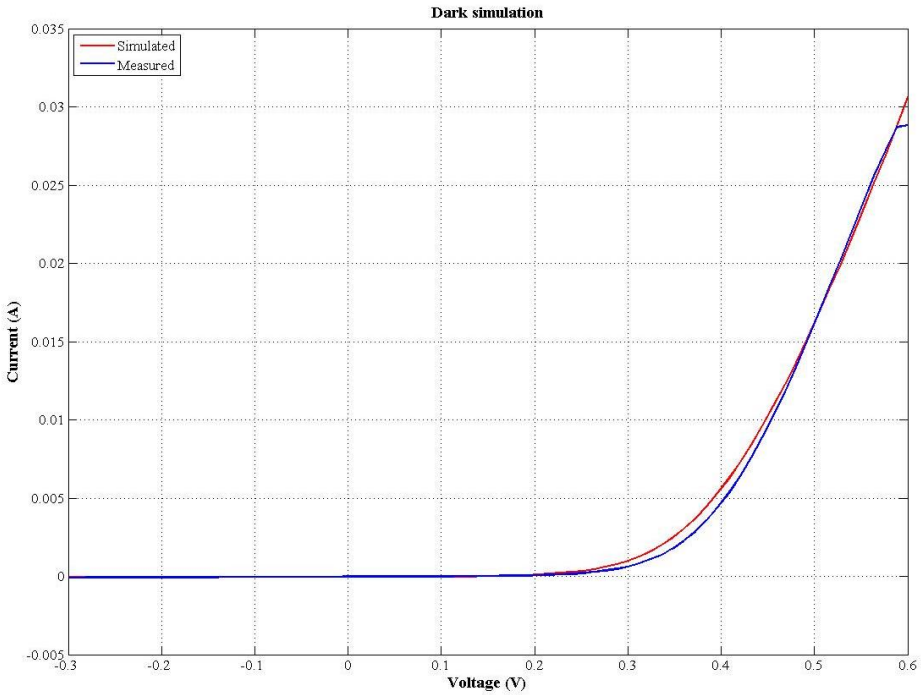

***Figure 12**: Dark simulation of cell 3.*

Cell 3	Light	Dark
RMSE (mA)	0.443	0.397
RMSE (%)	2.5	2.2

Table 8: RMSE of cell 3 simulation.

2.1.4.4 – Cell 4

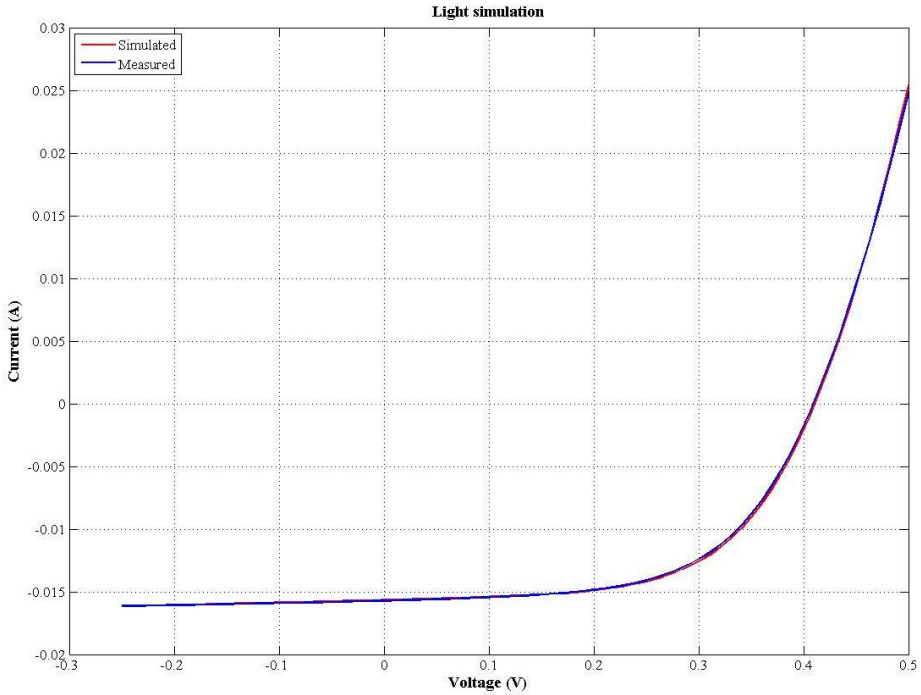

***Figure 13**: Light simulation of cell 4.*

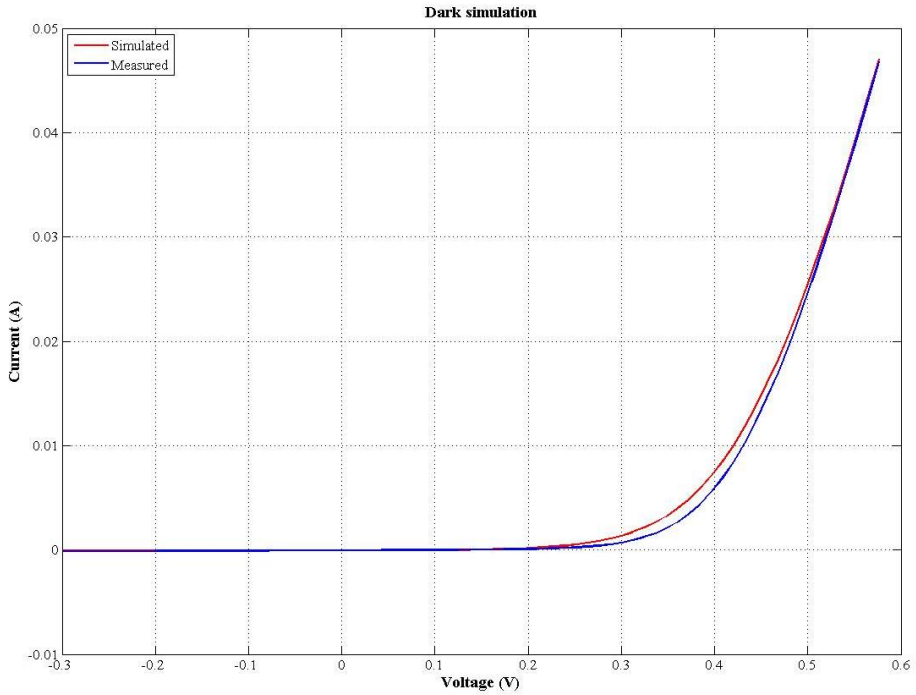

***Figure 14**: Dark simulation of cell 4.*

Cell 4	Light	Dark
RMSE (mA)	0.159	0.638
RMSE (%)	1	4

Table 9: RMSE of cell 4 simulation.

2.1.4.5 – Cell 5

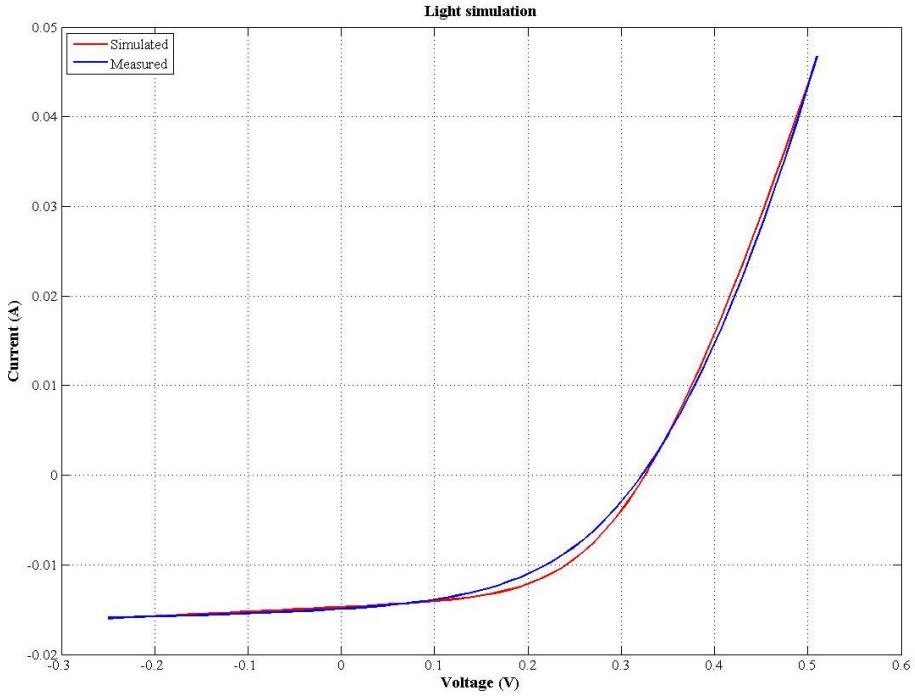

***Figure 15**: Light simulation of cell 5.*

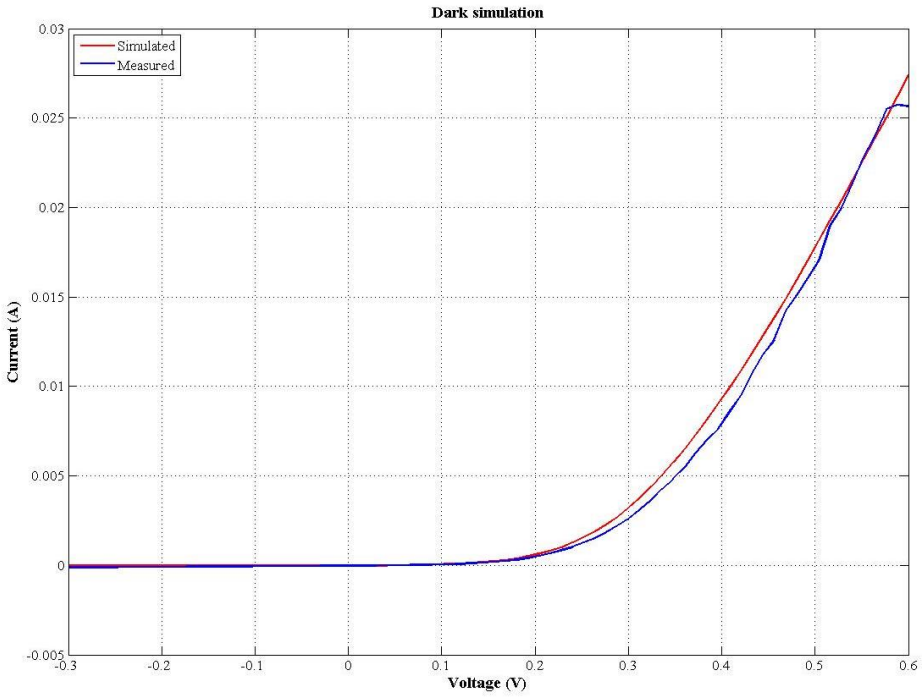

***Figure 16**: Dark simulation of cell 5.*

Cell 5	Light	Dark
RMSE (mA)	0.712	0.554
RMSE (%)	4.8	3.7

Table 10: RMSE of cell 5 simulation.

2.1.4.6 – Cell 6

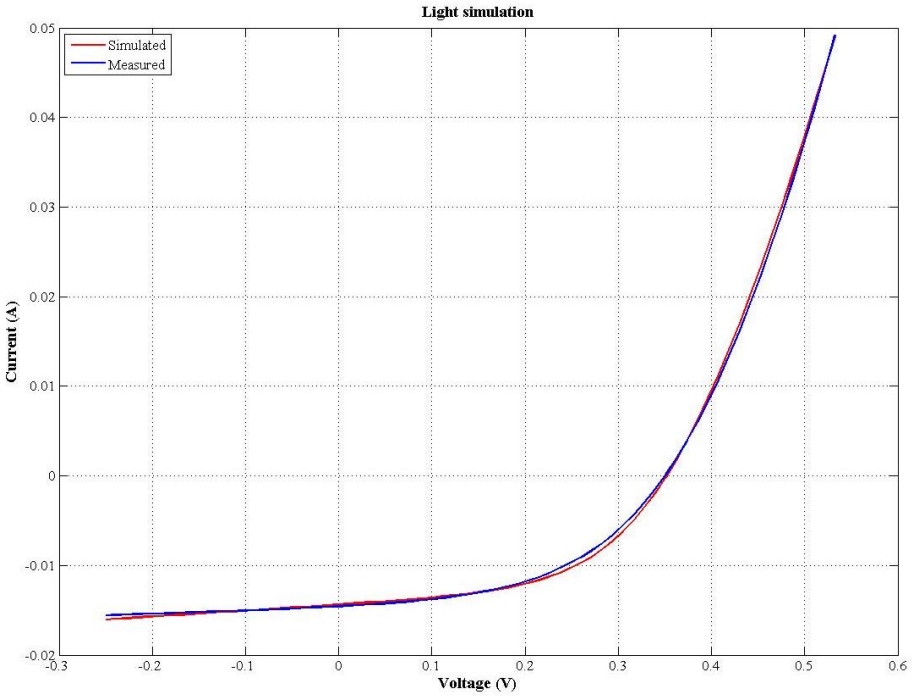

***Figure 17**: Light simulation of cell 6.*

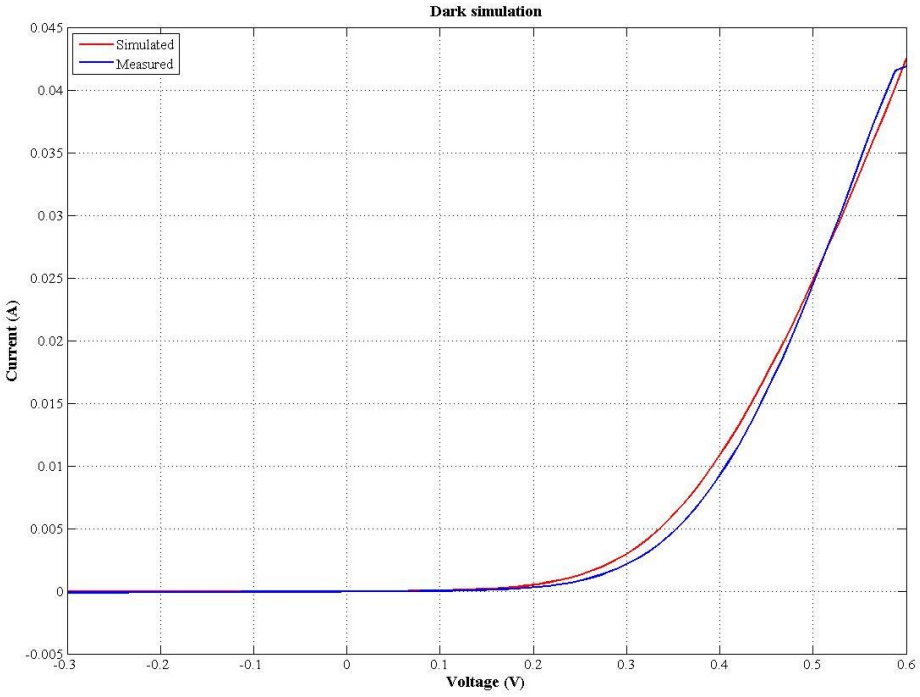

***Figure 18**: Dark simulation of cell 6.*

Cell 6	Light	Dark
RMSE (mA)	0.42	0.70
RMSE (%)	2.9	4.8

Table 11: RMSE of cell 6 simulation.

2.1.4.7 – Cell 7

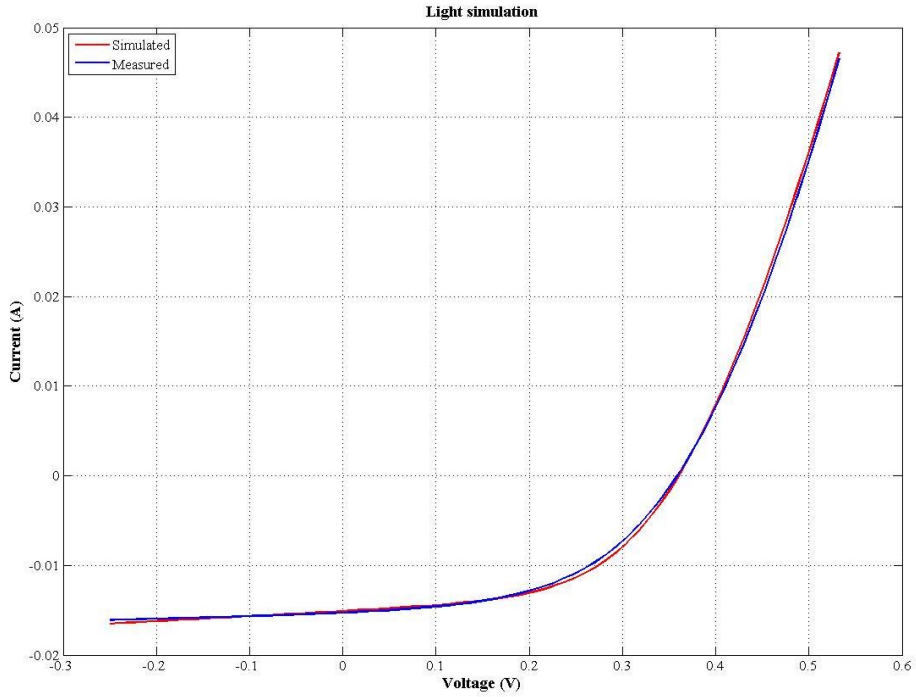

***Figure 19**: Light simulation of cell 7.*

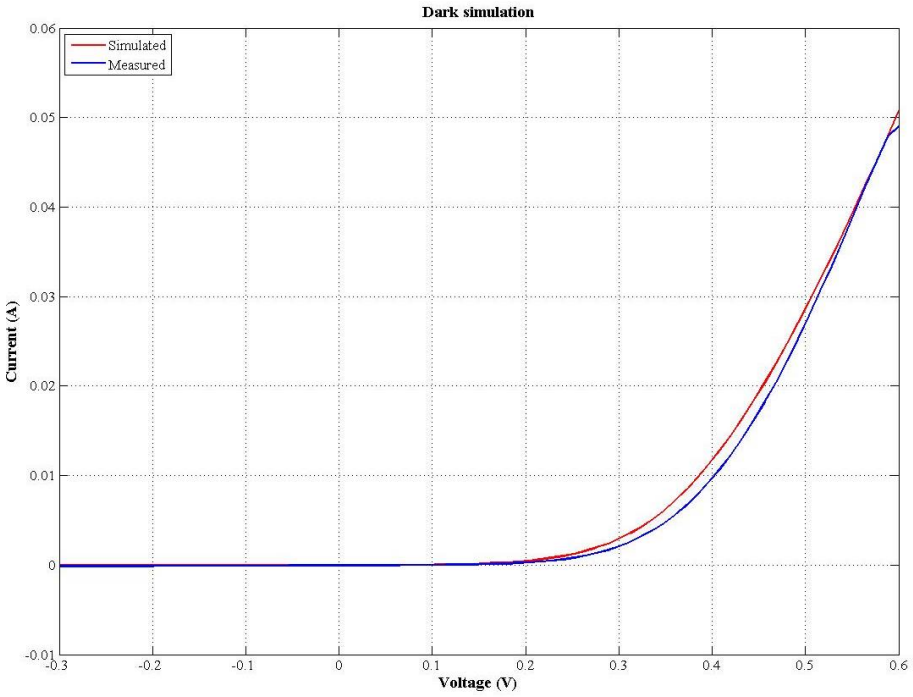

***Figure 20**: Dark simulation of cell 7.*

Cell 7	Light	Dark
RMSE (mA)	0.44	0.91
RMSE (%)	2.9	6

Table 12: RMSE of cell 7 simulation.

2.1.4.8 – Cell 8

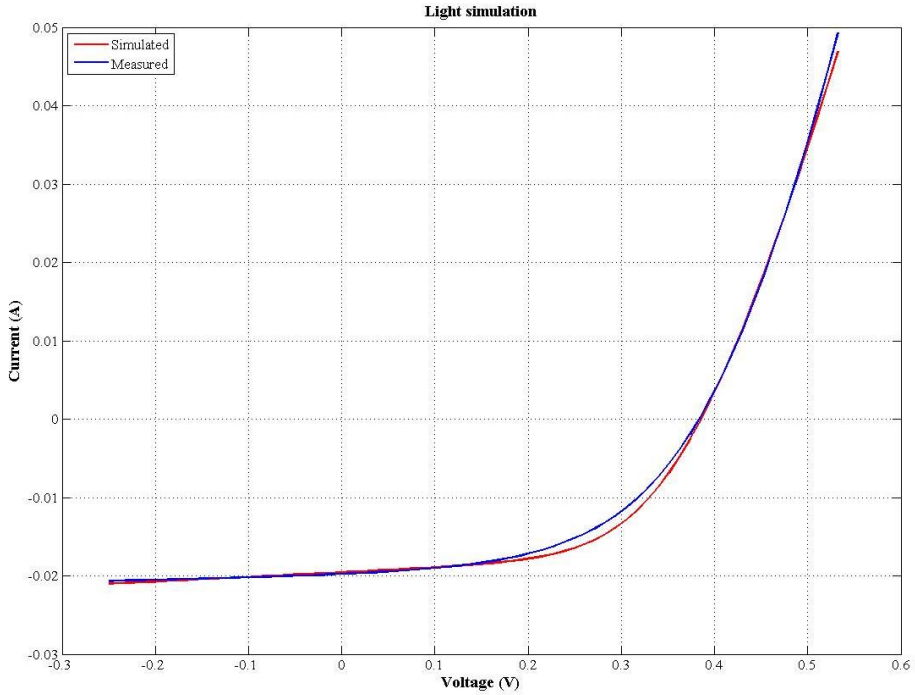

***Figure 21**: Light simulation of cell 8.*

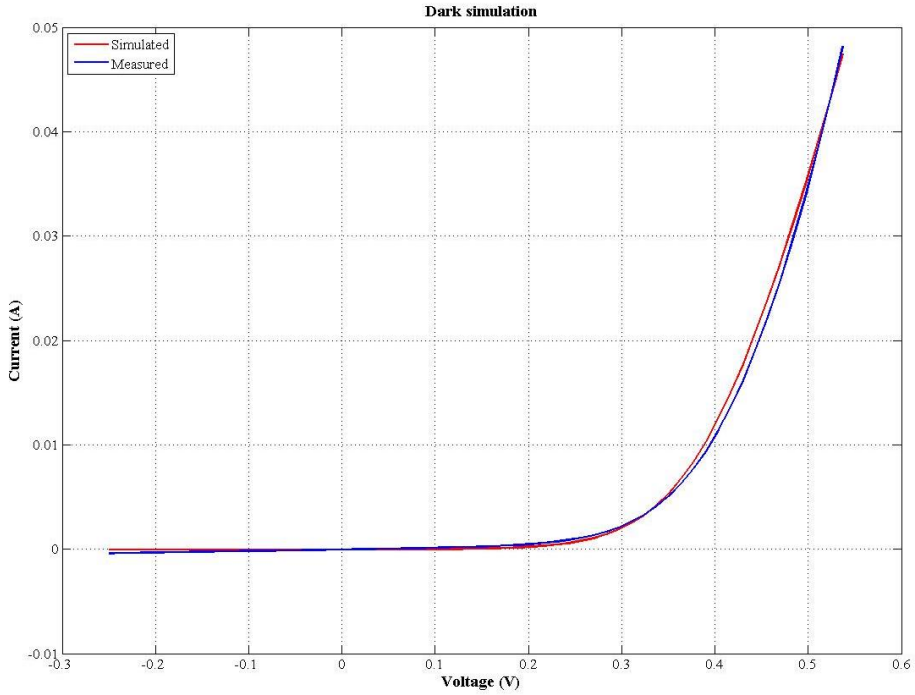

***Figure 22**: Dark simulation of cell 8.*

Cell 8	Light	Dark
RMSE (mA)	0.725	0.595
RMSE (%)	3.7	3

Table 13: RMSE of cell 8 simulation.

2.1.4.9 – Cell 9

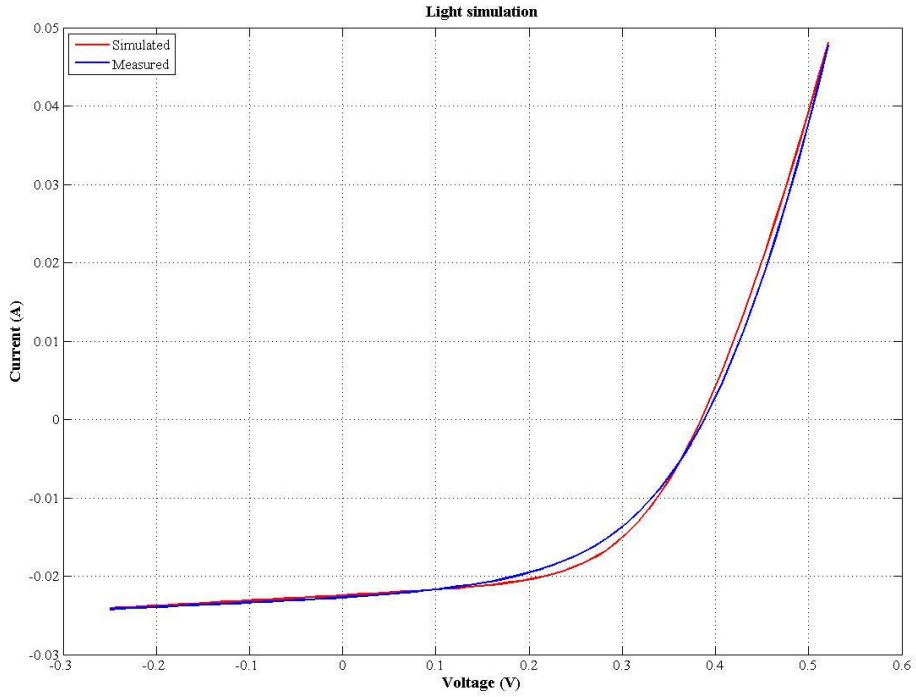

***Figure 23**: Light simulation of cell 9.*

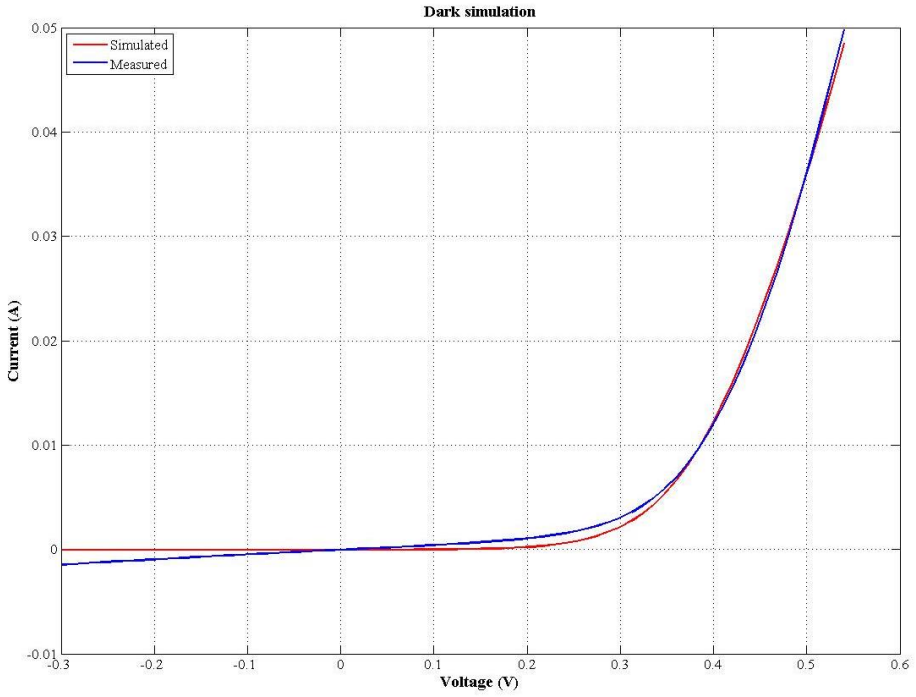

***Figure 24**: Dark simulation of cell 9.*

Cell 9	Light	Dark
RMSE (mA)	0.967	0.712
RMSE (%)	4.3	3.1

Table 14: RMSE of cell 9 simulation.

2.1.4.10 – Cell 10

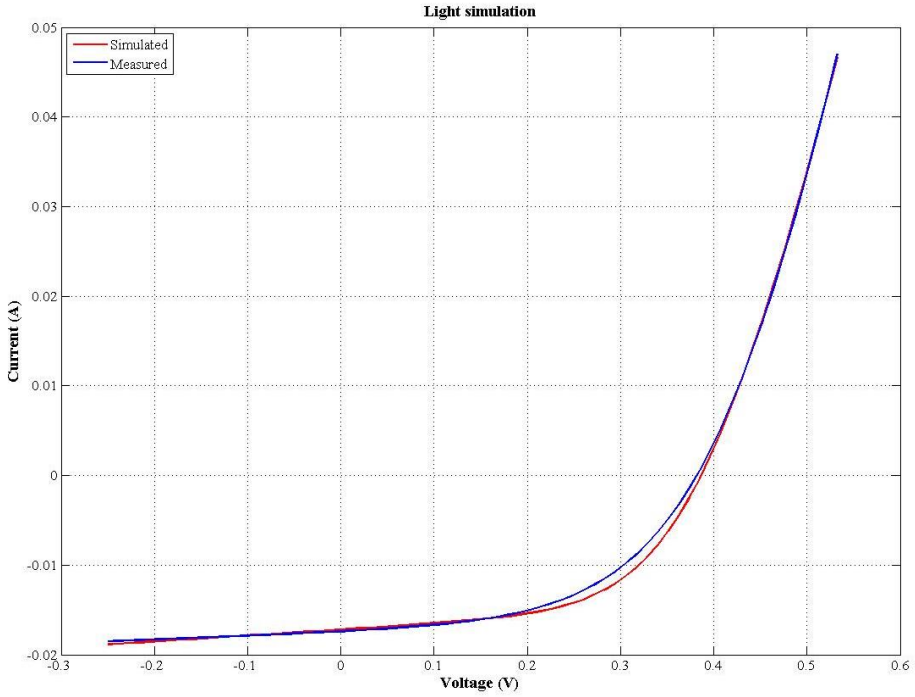

***Figure 25**: Light simulation of cell 10.*

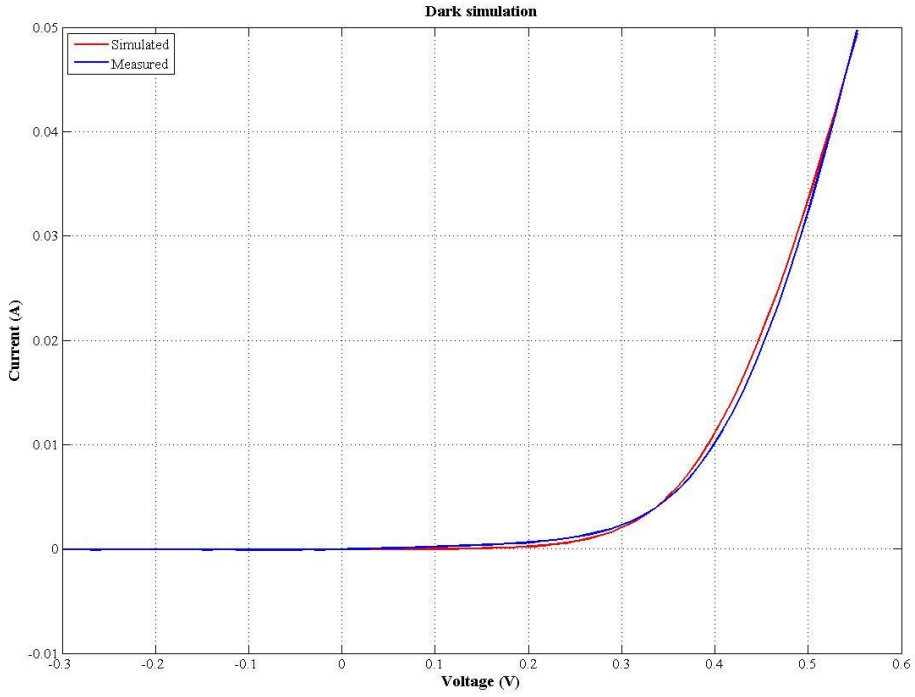

***Figure 26**: Dark simulation of cell 10.*

Cell 10	Light	Dark
RMSE (mA)	0.593	0.531
RMSE (%)	3.4	3.1

Table 15: RMSE of cell 10 simulation.

As it can be seen, the fitting is very good almost in all the simulations. In any case, it could be interesting commenting some details.

As already said, in some simulations, very few ones in fact, the final RMSE reaches a relative high value. In particular it happens for the solar cell number 9. In this case, looking at the light simulation, it is clear that the two curves have different slopes. Considering the mathematical shape of the governing equation, it is assumed that it is related to the exponential term. It means that the real value of the ideality factor "n" could be different with respect to the one used in the simulation. However, a better fitting has been not achieved and it is easy to think that maybe the reason has to be researched in the model used for the simulation.

Then, some interesting comments can also come from the solar cell number 7. In this case, a very good fitting has been achieved for the light condition simulation. On the other hand, the dark simulation ended with a RMSE relatively high. Probably it should be related to intrinsic characteristics of the cell that could cause little changes in the internal resistances, due to the exposure or not to the sun radiation, and as a consequence the little deviation that is observed.

Later, the behaviour of the measured dark I-V curve of the cell number 5 is very irregular. Probably, the reason why it happens is related to little problems during the measuring procedure.

Finally, the very best fitting has been performed for the cells number 2 and 4. In particular, referring to the light simulation, the RMSE turns out to be in the order of 0.2 and 0.1 mA respectively. Looking to the cell's characterization, it is evident that these two cells are the two best performing ones, in particular in terms of efficiency and fill factor. That could be not random.

2.1.5 - EQE measurements and cell characterization

The quantum efficiency (QE) is one of the most important magnitude useful to describe the features and goodness of a solar cell. More in details, it gives the number of electrons output by the solar cell, in comparison to the number of photon incident on the device.

Two different quantum efficiencies can be determined: internal (IQE) and external (EQE). The former is calculated taking into account only the non-reflected part of the incident spectrum, whereas the latter is computed considering the total spectral irradiance [11].
The calculation is according the equations (5) and (6):

$$IQE = \frac{J_{sc\lambda}}{q\phi_0(1-R)} \quad (5)$$

$$EQE = \frac{J_{sc\lambda}}{q\phi_0} \quad (6)$$

The parameters which affect them are:

- $J_{sc\lambda}$, the short circuit current density, dependent by the wavelength;
- q, the elementary charge;
- ϕ_0, the spectral photon flux;
- R, the reflection.

Both the internal and external quantum efficiencies depend on the wavelength.
It is clear that the QE affects a lot the performance of a solar cell. Moreover, one of the goals of this study is also to characterize the solar cells that are going to use. So, to ensure that the procedure has been going in the right way and that the obtained results are reasonable, the knowledge of the QE as a function of the wavelength could be one of the strongest tools, and soon it will be clear.
For this reason, the data about EQE provided by the IREC were very useful. However, not all the investigated solar cells correspond with the ones previously described, but the general structure is the same as well as the absorber layer composition, which is the one that mostly affects the cell's behaviour. Moreover, it has been noticed that for all the cells, the results of the measurements are really close one to each other, so it follows the evidence of a general behaviour for the whole family of kesterite solar cells.
Some examples of those measurements will be presented soon, by mean of several pictures. They show some plots of the quantum efficiency as a function of the wavelength. To build them, the data provided by IREC have been used. The wavelength range is between 300 nm and 1400 nm. In fact, outside from those values, the QE efficiency is almost zero.

Then, as already said, the results are really close for the all cells that have suffered measurements, so to avoid useless and boring repetition, just four out of eight graphs have been reported.

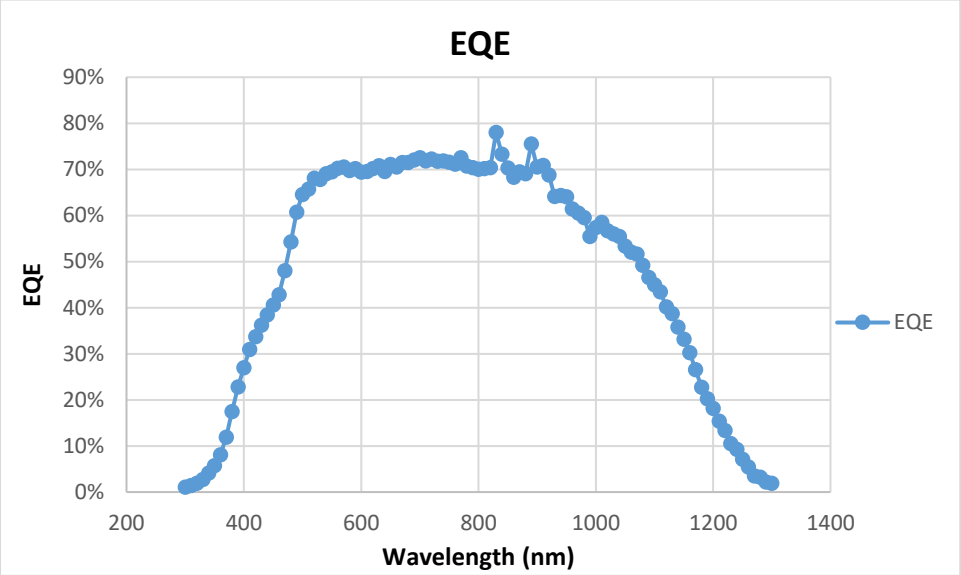

***Figure 27**: EQE, measurement 1.*

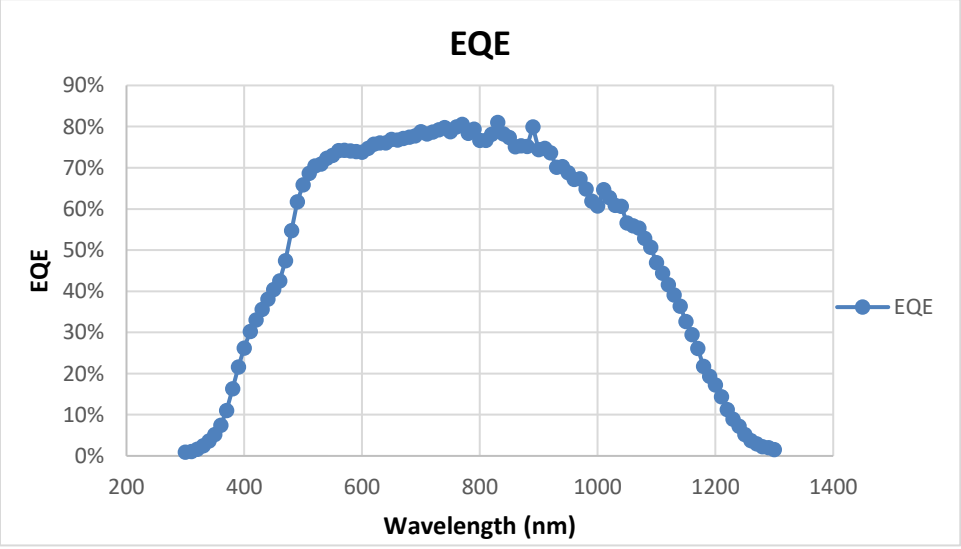

***Figure 28**: EQE, measurement 2.*

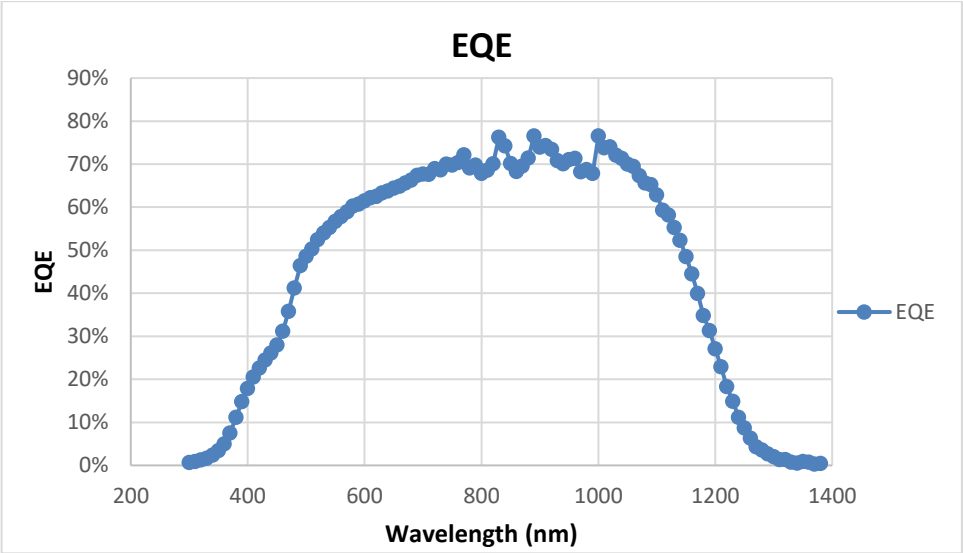

***Figure 29**: EQE, measurement 3.*

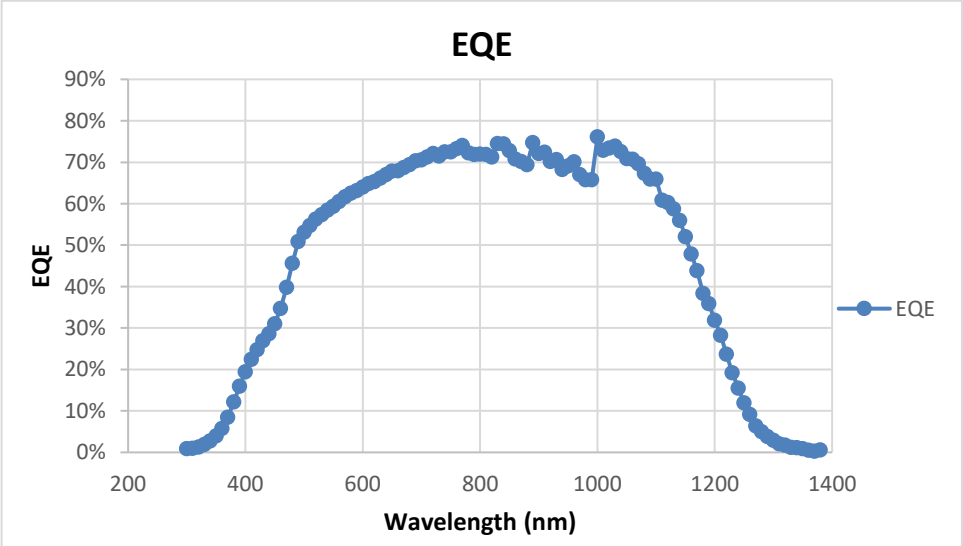

***Figure 30**: EQE, measurement 4.*

As it can be seen in figures 27, 28, 29 and 30, with few differences from one cell to another, the real useful spectrum range is between 500 nm and 1100 nm. In this range the quantum efficiency is higher than approximately 60%. Outside from this range, the quantum efficiency drops very suddenly.

Regarding the quality of the cells, to be honest, they are not good cells. In fact, the quantum efficiency never reaches values higher than 80%, except for very few points in the second example showed.

On the other hand, it means that a considerable amount of photons will be able to cross over the kesterite solar cell without being absorbed. It is not a bad news, considering what the goal is. In fact, the scope of this work is to build and analyse a tandem configuration of solar cells. The top one will be the kesterite based one, while the bottom one will be silicon based. The c-Si cell has very good performance, and also high quantum efficiency over a quite long wavelength range. It follows that if the amount of radiation reaching the bottom cell is still large, the c-Si cell will be able to work at a good rate. For sure not the best possible one, but neither so bad. In any case, these hypothesis will find a proof, or maybe not, only after the tandem configuration simulation.

Coming back to the data analysis, these measurements are now exploited to determine the short circuit current density, by mean of the EQE equation. This step is useful in particular to check if the characterization already done is correct.

So, knowing that:

$$J_{sc\lambda} = EQEq\phi_0 \tag{7}$$

And that:

$$J_{sc} = \int_0^\infty J_{sc\lambda} d\lambda \tag{8}$$

It follows that the short circuit current density can be calculated by the following integral [15]:

$$J_{sc} = \int_0^\infty (q\phi_0 EQE) d\lambda \tag{9}$$

The elementary charge is a well known constant, the spectral photon flux depends by the wavelength, as well as the EQE whose values have been provided.

For each measured value of EQE, corresponding to a certain wavelength, the product of the three magnitudes has been evaluated. Later, the integral has been solved by mean of a Matlab script using the Matlab function “trapz”. More in details, this function compute the integral of a quantity “Y” (the short circuit current density, in our case) with respect to a quantity “X” (the wavelength spectral range) using the trapezoidal method.

At the end of the procedure, the results showed values of the short circuit current densities in the range between 25 and 28.5 mA/cm^2, for the several cells whose EQE's measurements have been provided.

We already said that not all the data are referred to the same ten solar cells previously characterized. However, for both the solar cells number 3 and 4, during the parameter's extraction procedure it has been obtained a short circuit current density of 28 mA/cm^2. In this last step, using the EQE equation, for both cells a short circuit current density of 27.14 mA/cm^2 emerged. The results are not the same, since they come from different procedure. However, they are really close, and due to this, it is assumed that both the calculation are right. As a consequence, there are no reasons to not assume as exact also the characterization performed for all the other kesterite based solar cells.

2.2 – c-Si solar cell

C-Si is referred to as the crystalline forms of silicon. Two alternatives exist: mono-crystalline silicon, consisting of a continuous crystal, or multi-crystalline silicon, consisting of small crystals.

This technology has been developing since 1950s. For this reason, solar cells made of crystalline silicon are often called as conventional, traditional, or first generation solar cells. Moreover, from the beginning of its development and production, c-Si is the most common material used in that field [3].

C-Si based solar cells are usually single-junction cells, in opposition to the multi-junction, and generally more efficient than the other technologies, such as the second generation thin film solar cells, among which, CdTe, CIGS and amorphous silicon are the most common ones. Just as a clarification, the amorphous silicon is not considered as a crystalline material due to its unordered amorphous (without shape) structure.

The efficiency of these devices can reach values of 26.7% and 21.9% for mono-Si cells and multi-Si cells respectively [4]. Of course these are values reached in lab condition, while during commercial application the performances are worse. However it indicates that the conventional silicon technology still had the potential to improve and therefore to maintain its leading position among the several technologies in the market share.

Then, one more important concept is the energy payback time (EPBT). It describes the time the solar cell need to produce the same amount of energy used for its production. In the last decades, this time has been reduced a lot, making solar photovoltaic application a very mature and also convenient technology. In any case, it depends by the location where the PV systems are installed and the specific PV technology implemented. Among the c-Si solar cells, it has already been said that two main categories are available. The mono-crystalline solar cells are more efficient than multi-crystalline ones, but they require expensive and energy demanding procedure. The most common method to produce mono-crystalline silicon wafers is the Czochralski Growth method. To give an idea, as an order of magnitude, in 2009 it accounted for approximately 50% of the final price of the product [12]. With development and new technologies, its impact is surely lower but it still remains the main cost demanding step for the mono crystalline cells production. This is why, even if multi-crystalline solar cells are a bit less efficient, they are anyhow the most relevant technology in the market share, leading to a shorter EPBT.

2.2.1 - Fabrication process

Interdigitated back contact (IBC) solar cells were manufactured using high quality FZ <100> c-Si(p) 4" wafers with resistivity and thickness of 2.5±0.3 Ωcm and 280±20 µm respectively.

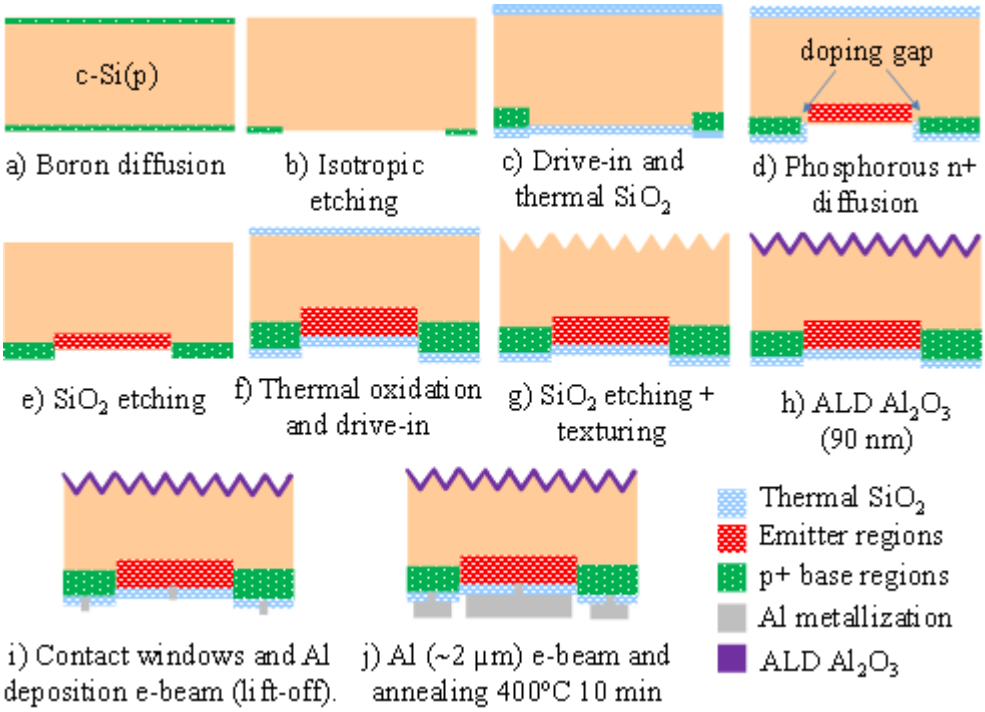

***Figure 31**: Main stages of the baseline fabrication process with homogeneous emitter [14].*

Cells were fabricated using the flow process shown in Figure 31, considering next main technological features, namely: 1) boron and phosphorous diffusions to form p+ (base contacts) and n+ (emitter regions) regions respectively, which are patterned using standard photolithography. 2) A front surface textured with random pyramids and passivated with 90 nm ALD Al_2O_3 films, resulting reflectance values below 0.5% at wavelengths λ~600 nm with effective surface recombination velocities below 3 cm/s (@ 1Sun). 3) A back reflector scheme consisting of a thermal SiO_2 (110 nm)/Al (~2 µm) stack was included at the rear side [13].

2.2.2 - Real I-V's measurements and cell characterization

As it happened for the kesterite solar cell, even for the silicon one the I-V measurements have been provided, both in light STC and dark condition.

The goal is again to achieve the most important parameters that characterize the solar cell it is going to be used in the final tandem configuration, in order to get a clear idea about its performances and to predict what could be its behaviour during operation. Moreover, these results will be used also to determine if the tandem configuration allows reaching better performances with respect to the single c-Si cell, since this is our objective.

Furthermore, the silicon solar cell will be deeply analysed. In particular, it will be attempted to model it and to extract the parameters that describe the model used in the analysis and, consequently, that determine the results will be got. It follows that the real I-V measurements are the strongest tool through which the simulated results can be compared and eventually validated. However, for the silicon technology, just one cell has been studied, since it is a very mature technology. So, focusing on the light measurements, the following parameters will be got: the open circuit voltage, the short circuit current, the fill factor and the solar cell efficiency. Since they are the same obtained for the kesterite solar cell, it is avoided to repeat the explanation about the physical meaning of each one of them.

Just as a reminder, it could be useful to remember how the fill factor (FF) and the efficiency (η) are obtained:

- $FF = \frac{V_m I_m}{V_{oc} I_{sc}}$ (1)

- $\eta = \frac{I_m V_m}{G_{STC} A}$ (2)

The results are summarized in table 16.

Solar cell	c-Si
Isc(mA)	368.6
Voc(mV)	647
Im(mA)	343
Vm(mV)	532
η(%)	20.275
FF	0.765
Area(cm^2)	9

Table 16: c-Si solar cell characterization.

2.2.3 - Parameters extraction

Even for the silicon solar cell, the procedure continues determining the parameters which describe the "five parameter model" [9].

The governing equation is the same used for the kesterite solar cells (equation 3):

$$I_{cell} = I_{ph} - I_0 \left[e^{\frac{V_{cell} + I_{cell} R_s}{n V_T}} - 1 \right] - \frac{V_{cell} + I_{cell} R_s}{R_p} \quad (3)$$

As a reminder, we know that the several factors are:

- I_{cell}: the output current of the solar cell;
- V_{cell}: the output voltage of the cell;
- I_{ph}: the photo-generated current;
- I_0: the diode reverse saturation current;
- n: the diode ideality factor;
- V_T: the thermal voltage;
- R_s: the series resistance;
- R_p: the shunt resistance.

Once again, the parameters of the model are investigated: the short circuit current density "Jsc", the series resistance "Rs", the shunt resistance "Rp", the ideality factor "n" and the

saturation current "I_0". They are the factors that mainly affect the I-V curve's shape and it is the reason why the modelling procedure cannot overlook their resolution.

Now, to get them it was followed a different way with respect to the algorithm used for the kesterite solar cell.

In fact, different software has been exploited: PSpice [11].

By mean of this tool, it is possible to build an equivalent circuit corresponding to the solar cell is going to be studied. PSpice asked for some parameters, such as the Sun irradiance, the cell area, and some universal constants like the Boltzmann one and the elementary charge. Moreover, it is required to put an initial value for each one of the five parameters.

At this point, the simulation can start and the results are shown. Obviously, the main interest is again on the I-V curve because it will be used to compare the simulated with the measured data.

So, if the results were very far from the real measured data, some parameters had to be modify, and the simulation run again, otherwise, if suitable results are achieved, the five parameters are saved and it starts the comparison of the simulated results with the measured ones, in order to validate them.

Finally, the values are shown in table 17.

Solar cell	**c-Si**
Jsc(mA/cm^2)	40.95
Rs(Ohm)	0.11
Rp(Ohm)	4500
n	1.12
I_0(A)	7.6831 10^{-11}

Table 17: c-Si solar cell's five parameters.

2.2.4 - Validation and comparison between real and simulated data

The next step, i.e. the validation of the simulated data has been performed following the same procedure of the kesterite solar cells.

So, the simulated current data have been compared with the measurements and the RMSE has been calculated. The check has been done for both light and dark condition.

At the end of the procedure it is expected to validate the results, but to do that, it must be satisfied the constraint that the RMSE is lower enough. Remembering that it is calculated according the equation 4:

$$RMSE = \sqrt{\frac{\sum_{t=1}^{n}(y_m - y_s)^2}{n}} \quad (4)$$

Where:

- y_m is the measured value;
- y_s is the simulated value;
- n is the number of point.

At the end of the analysis, the following results have been got (Fig. 32 and Fig. 33).

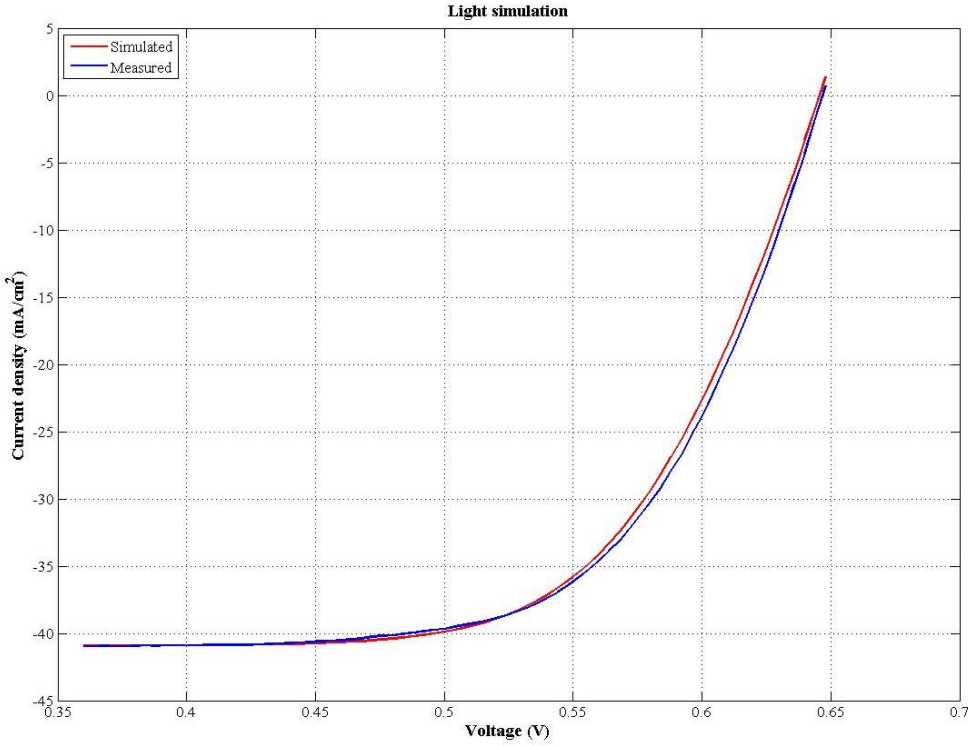

***Figure 32**: Light simulation of c-Si solar cell.*

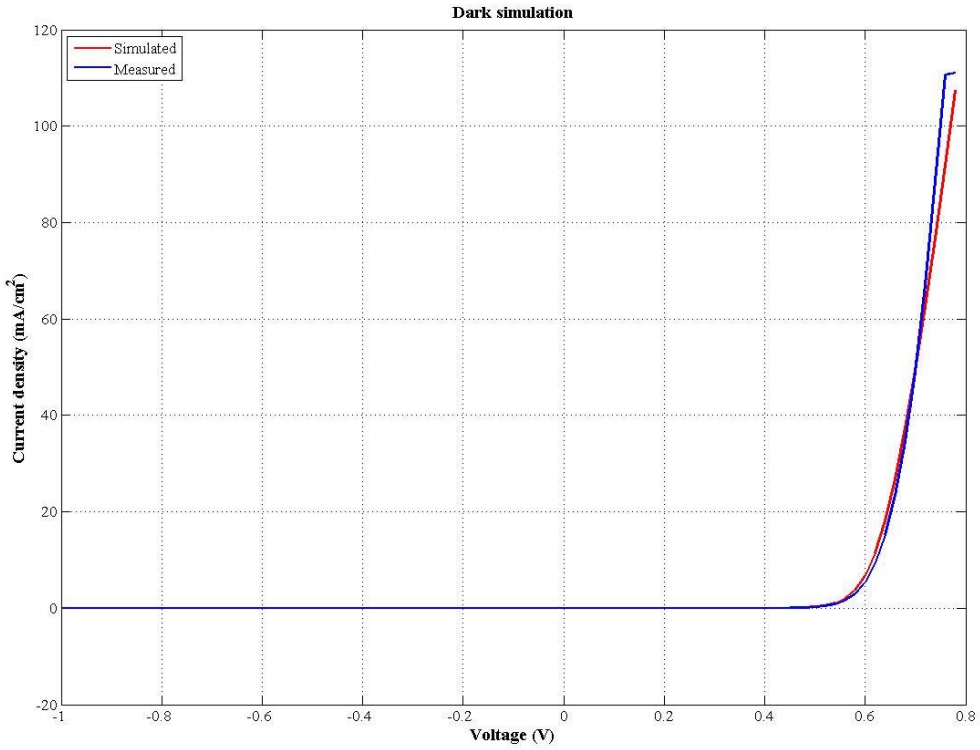

***Figure 33**: Dark simulation of c-Si solar cell.*

c-Si solar cell	Light	Dark
RMSE (mA/cm^2)	0.592	2.49
RMSE (mA)	5.333	22.452
RMSE (%)	1.4	6

Table 18: RMSE of c-Si solar cell simulation.

As it can be seen, the fitting between measured and simulated results is very good. Nevertheless, the RMSE is not as low as for the kesterite solar cells. However it is also clear that the c-Si cell is characterized by a much higher short circuit current, and it should be taken into account while validating the results. It follows that in terms of percentage, the RMSE is really good, since the error related to the light condition simulation is much lower than the 5% (the chosen threshold) of the Isc (almost 1.5%). Finally, the behaviour of the simulated I-V curves matches so good the measured ones. For these reasons, it can be stated that the c-Si solar cell has been well characterized.

2.2.5 - EQE measurements and cell characterization

As it happened for the kesterite based solar cells, also data about the EQE of the c-Si solar cell are available. So, the idea is to follow the same procedure performed for the top cell: exploiting the EQE measurements, and its equation, to determine the short circuit current density of the cell, and successively comparing it with the value obtained during the characterization step in order to ensure that the analysis has been performed correctly, leading to the right results. Those measurements are now shown, by mean of a plot. On the vertical axis there is the wavelength spectrum range which goes from 200 nm until 1400 nm, even if data are available only between 300 and 1200 nm. On the vertical axis, instead, the EQE is reported, in decimal format (instead of percentage).

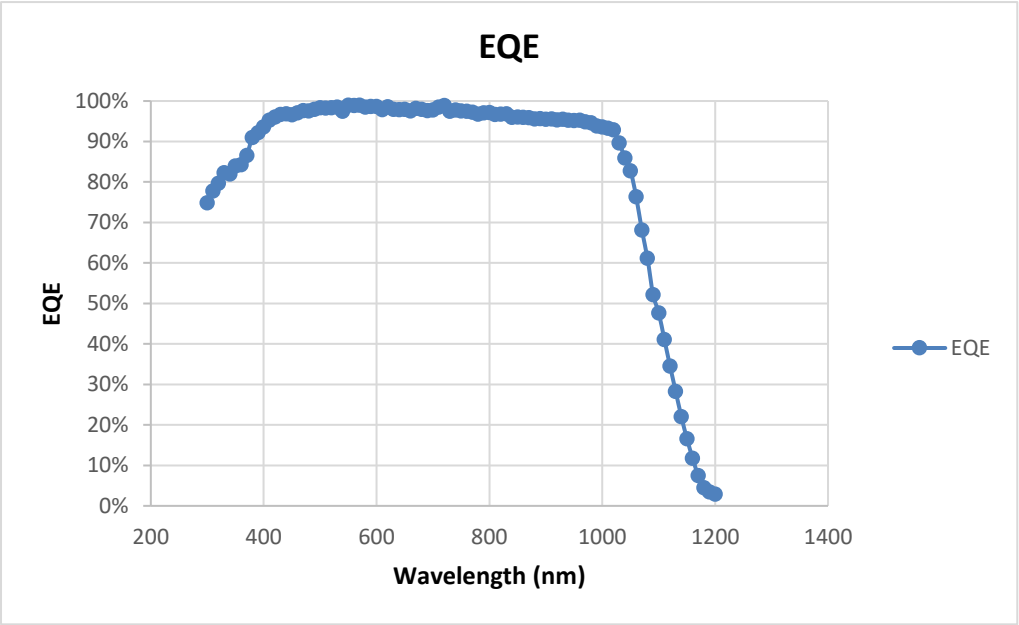

***Figure 34**: c-Si solar cell's EQE.*

Comparing with the results of the kesterite solar cells, it is evident that the quality of the cell is much higher for the c-Si solar cell. It is highlighted by the huge value of the quantum efficiency, especially for wavelength between 400 and 1000 nm. In that range it is well above 90%, allowing the cell to absorb a huge amount of photons, and consequently producing a good current, which however depends also by others factors.

In any case, as already introduced before, it remembers that the performance of that bottom cell will depend by the characteristics of the top one, so, the absorbance of the c-Si will effectively change.

Coming back to the primary goal of this step, it will now be tried to obtain the short circuit current density. The equation 9 will be used, as well as the same procedure and algorithm, employed for the kesterite cells.

As a reminder, equation 9 is:

$$J_{sc} = \int_0^{\infty} (q\phi_0 EQE) d\lambda \quad (9)$$

At the end of the simulation of the Matlab script, it is got a short circuit current of 39.42 mA/cm^2. Matlab environment has been widely used in the simulation of photovoltaic devices [16-17].

Even in this case, the result is just a bit different from what got during the characterization. The reason is due to the performed procedures. During characterization, the real I-V measurements have been used, while during this step EQE measurements were exploited. However, they could suffer little measuring errors. This is what probably happened. Moreover, the common way to work with EQE is to know the short circuit current of the solar cell and then to adjust the measured data in order to match them. Now the opposite method has been followed. In fact, the EQE measurements were directly used to determine the short circuit current density. Anyway, the results are in the same order of magnitude, and the relative error between them is quite small. So it can be stated the results achieved until now find a proof.

3. Simulation of tandem characteristics

Once both the solar cell technologies have been studied and well characterized, they can be used for the next steps. As already mentioned, the goal of this work is to build a tandem configuration of two solar cells and to simulate its behaviour in order to evaluate the performances. For obvious reasons, particularly related to physical properties, the top cell of the tandem will be the kesterite one, while the c-Si solar cell will be set as bottom cell. Entering more in to details, in order to exploit reasonably both the cell's capabilities, it is needed that some photons (and their energy) pass through the top cell, reaching the bottom one. The c-Si has a very high EQE in a wide spectral range and it probably means that it would absorb almost all the photons reducing dramatically the already bad performances of the kesterite based solar cell, if it was installed on the bottom of the tandem. So the opposite configuration has been chosen. Unfortunately, looking at the EQE measurements (figures 27, 28, 29, 30 and 34) it is evident that the solar cells have similar energy bandgap. It means that they should absorb almost in the same range, preventing the optimal behaviour of the configuration. However, before taking cure about the optical properties, it is intended to simulate the tandem configuration.

3.1 – Electronic circuit

To perform the electrical simulation of the tandem configuration, PSpice has been used again. It is a software developed in C language, which allows to create an electronic circuit according to the input setup [11].

In the specific case study, the solar cells have been analysed by mean of the five parameter model [9]. It follows that the electrical circuit deriving from this model has to be implemented for both the cells, in order to create a connection. PSpice is able to do it just handling the relationship between the several nodes of the circuit, which are introduced by the user. At the end, the goal is to connect the two cells in series. So, the resulting electronic circuit is shown in figure 35.

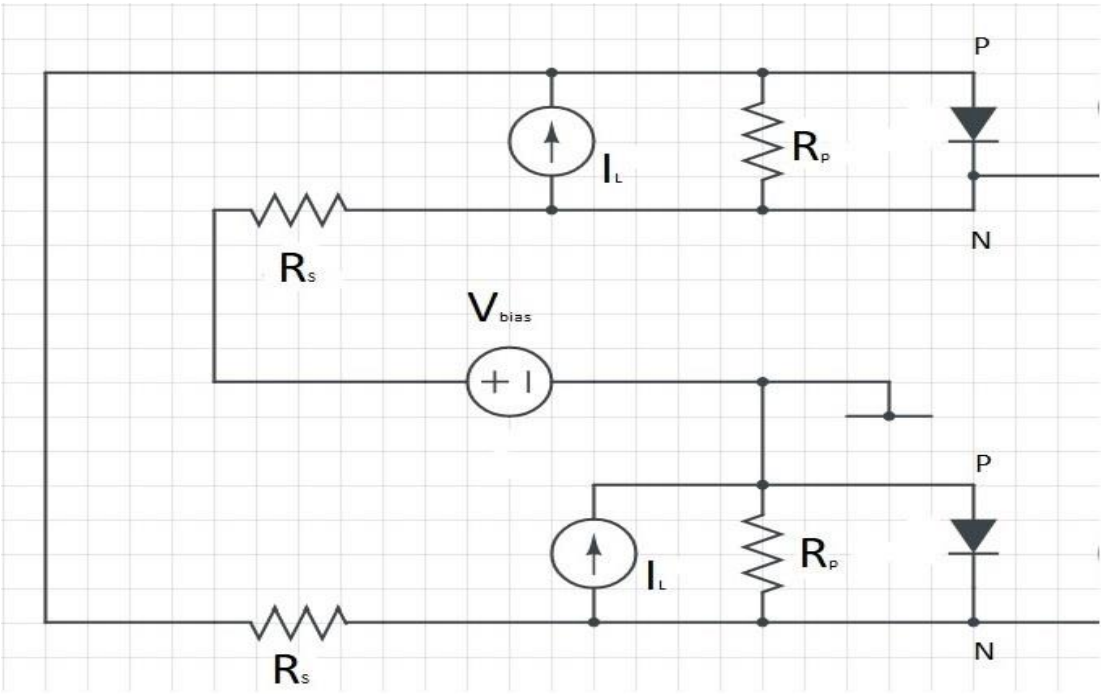

***Figure 35**: Electronic circuit of the tandem.*

Looking at the circuit, since the connection is in series, it follows that the total voltage output will be almost equal to the sum of the voltage of the two cells, while the current output will be limited by the worst performing one, which can be either the top or the bottom cell, since it depends by the working conditions.

3.2 – PSpice simulation

After having defined the connection between the nodes and the cell, i.e. the electronic circuit, the simulation can start.

In particular, the interest is focused on analysing how the efficiency of the tandem changes with the variation of the bottom cell current density. In fact, while the top cell should behave like described during the parametrization, since it is not affected by any obstacle, the bottom cell will be affected by the top one through its absorptivity and transmissivity. This situation will be reflected in the variation of the short circuit current density of the c-Si cell, i.e. the maximum achievable one. This analysis will be performed for the several solar kesterite based solar cells, also in order to see if a general behaviour occurs, but in particular, to check which ones allow the best performances, so to focus on them during

further eventual research and developments. Then, all the others needed parameters are known. For both the cell's technologies, they are the same found during the parameters extraction step plus the voltage determined during the characterization. In any case, they will be kept fixed during the simulation. Proceeding in this way, several curves will be obtained, each one referred to a particular tandem configuration among one kesterite based solar cell and the crystalline silicon one. As said, the key parameter is the bottom cell current density. During the simulation it will vary inside a range from 2 until 44 mA/cm^2. The thresholds delimit the whole possible working condition range, since 2 mA/cm^2 is a very low current density the cell can produce even with a very low photon absorption, while 44 mA/cm^2 is the theoretical maximum short circuit current density the c-Si would output if the EQE was 100% over the whole spectral range, but of course it is an unfeasible condition.

At each step the parameter is incremented by 3 mA/cm^2, giving a specific working point.

What it is expected is that rising up the bottom cell current density, also the efficiency increases, since the current output is higher, while the voltage does not change, and the power depends by both voltage and current. The increasing should be almost linear. That is until the top cell current density value is reached. At this point, even increasing the bottom one, the tandem current density will be limited by the top one, due to the series connection. It follows that the efficiency would increase very slowly, in a logarithmic way, reaching an asymptote really soon. An overview of the results is illustrated in figure 36.

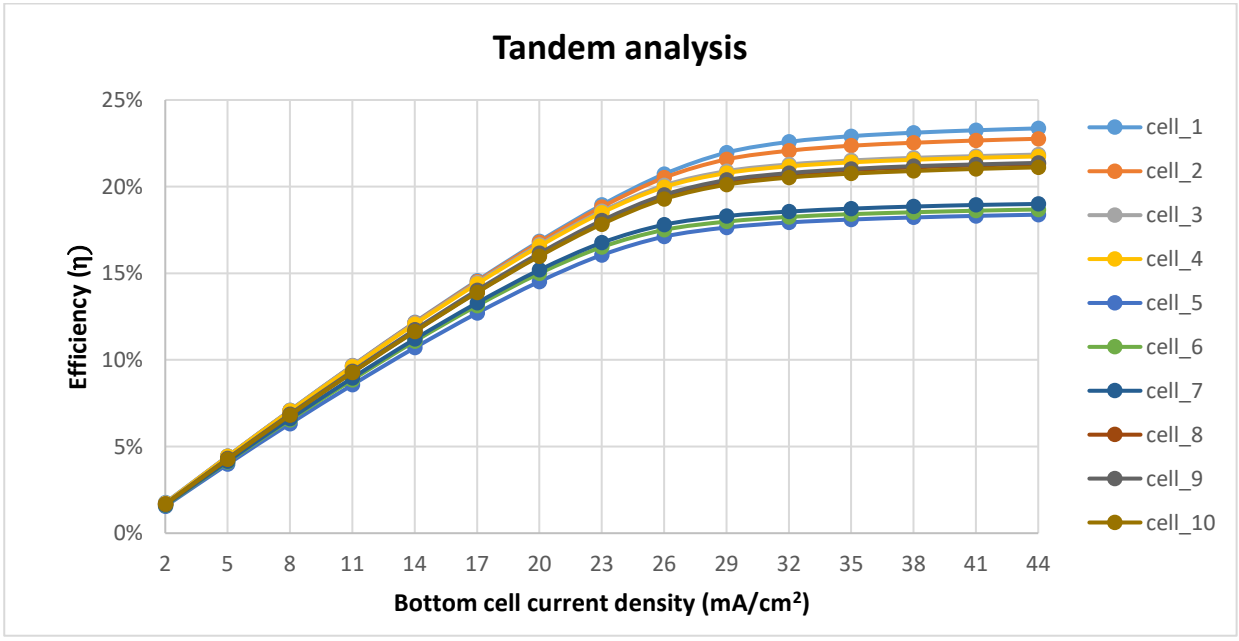

***Figure 36**: Tandem analysis.*

The picture shows that the results agree with the expectations, at least regarding the efficiency curves behaviour. Moreover, it is also visible how much the quality of the top cell affects the tandem performances. The bigger differences occurs at very high bottom cell current density, where they can be seen differences in efficiency in the order of 5 points percentage between the several possible tandems. In that condition, what mostly affects the results is the voltage output of the kesterite solar cell. So, cells with higher voltage output allow to reach higher power production and so higher efficiency. Going to the left side of the graph, instead, the curves are closer each other. There, the low current density output limit the efficiency reachable by all the cells.

Anyway, the aim of a tandem configuration is to achieve a higher efficiency with respect to the single cell working alone. The c-Si cell that has being used has an efficiency of almost 20%. In half the analysed cases, that limit can be exceeded, at least theoretically, since values higher than 23% have been achieved. In reality, it has to be remembered that the bottom cell current density will be limited by the optical properties of the top cell, therefore working conditions at very high values are not realistic.

In order to know what will be the actual working point of the tandem configuration, the optical properties of the top solar cells have to be measured. It would allow determining the filtered short circuit current density of the c-Si solar cell.

4. Conclusion

This work focused on the analysis of two solar cells technology, kesterite-based solar cell and crystalline silicon one, aiming to build a tandem configuration of them, and perform an electrical simulation of the tandem in order to analyse the expected efficiency of this topology.

In order to do that, the study could not overlook the modelling of the solar cells. After some evaluations, the "five parameter model" was selected, since it seemed the most suitable one for the purpose of this work.

So firstly, the several samples of kesterite-based solar cell have been modelled. By mean of mathematical algorithms implemented on Matlab environment, the model parameters extraction has been performed, allowing determining all the factors affecting the model. Then, for each one of the cells, the modelling procedure has been validated comparing the I-V curve resulting from the simulation with respect to the measured one, both in light and dark conditions. Since the good results obtained, it is stated that the "five parameter model" well describes the behaviour of this solar cell technology.

The same has been done for the c-Si solar cell, even if different software has been exploited: PSpice. In any case, at the end of the simulation, the I-V curve of the modelled cell is obtained, and by a comparison with the measured one, the parameters come to a validation. All these steps were needed to achieve the objective of this study that is the electrical simulation of tandem kesterite/c-Si solar cells in series configuration.

The simulations were performed using PSpice again, where the electronic circuit was built. In the configuration proposed in this study, the kesterite cell is set as top cell, while the c-Si one as bottom cell.

The results obtained show that making use of the best kesterite cell among the ten analysed, it is possible to achieve a tandem efficiency of 22.5% with a bottom cell short circuit current density of 32 mA/cm^2, which is achievable, at least theoretically, since the short circuit current density of the c-Si cell at STC is 40.95 mA/cm^2.

However, looking at the EQE measurements of the kesterite-based solar cells (Figures from 27 to 30), important optical losses can be observed. They are mainly due to high value of the frontal reflection. Moreover, the same measurements show that the two different absorber

layers (kesterite and c-Si) have a very similar bandgap, preventing the optimal tandem functioning.

So, in order to achieve high efficiency values of the tandem structure it is necessary to reduce these optical losses by minimizing the reflection of the TCO layer of the top cell and try to achieve high transmission of the kesterite absorber layer at high longwave values. This last goal can be meet increasing the band gap of the absorber layer, working on its chemical composition, for example raising up the sulphur over selenium ratio (S/Se).

Acknowledgments

This master thesis is the conclusion of a five years long period of university career that deeply characterized my person, improving my knowledge and giving the opportunity to meet great people. For this reason, I would like to thank those people who helped me to achieve this point of my life and to develop this work.

Therefore, foremost my family, for their sacrifices and their love. They supported me from the very beginning of my path, always advising the right way for everything.

I am grateful to Prof. Santiago Silvestre from Universitat Politècnica de Catalunya (UPC), who accepted to be the director and the supervisor of this work, for supporting me, with his patience and knowledge, without hesitation during the development of this thesis.

My sincere thanks also goes to Prof. Vittorio Verda from Politecnico di Torino, for his availability during all my Erasmus period at UPC and for his activity as tutor of the final master thesis together with the Prof. Filippo Spertino, from Politecnico di Torino again, to which my sincere thanks go too.

Then, I would like to express my gratitude also to Alejandro Hernández from IREC (Institut de Recerca en Energia de Catalunya) for his important role in providing data and technical information about solar cells.

Finally, thanks to Federica to be always there and for his support during hard moments and to my friends for their support again and for giving me their time.

References

[1] U.S Energy Information Administration (EIA). (2017). International Energy Outlook 2017.

[2] Karanfil, F., & Li, Y. (2015). Electricity consumption and economic growth: exploring panel-specific differences. *Energy Policy*, *82*, 264-277.

[3] Burger, B., Kiefer, K., Kost, C., Nold, S., Philipps, S., Preu, R., Rentsch, J., Schlegl, T., Stryi-Hipp, G., Warmuth, W., Willeke, G., Wirth, H. (2018). Photovoltaics Report.

[4] Green, M. A., Hishikawa, Y., Warta, W., Dunlop, E. D., Levi, D. H., Hohl-Ebinger, J., & Ho-Baillie, A. W. (2017). Solar cell efficiency tables (version 50). *Progress in Photovoltaics: Research and Applications*, *25*(7), 668-676.

[5] Mitzi, D. B., Gunawan, O., Todorov, T. K., Wang, K., & Guha, S. (2011). The path towards a high-performance solution-processed kesterite solar cell. *Solar Energy Materials and Solar Cells*, *95*(6), 1421-1436.

[6] Simya, O. K., Mahaboobbatcha, A., & Balachander, K. (2015). A comparative study on the performance of Kesterite based thin film solar cells using SCAPS simulation program. *Superlattices and Microstructures*, *82*, 248-261.

[7] Hernandez Martinez, A., Placidi, M., Arques, L., Giraldo, S., Sánchez, Y., Izquierdo-Roca, V., & Saucedo, E. (2018). Insights into the formation pathways of Cu2ZnSnSe4 using rapid thermal processes. *ACS Applied Energy Materials*.

[8] Barkhouse, D. A. R., Gunawan, O., Gokmen, T., Todorov, T. K., & Mitzi, D. B. (2012). Device characteristics of a 10.1% hydrazine-processed Cu2ZnSn (Se, S) 4 solar cell. *Progress in Photovoltaics: Research and Applications*, *20*(1), 6-11.

[9] Yahfdhou, A., Mahmoud, A. K., & Youm, I. (2016). Evaluation and determination of seven and five parameters of a photovoltaic generator by an iterative method. *arXiv preprint arXiv:1601.03257*.

[10] Aberle, A. G., Wenham, S. R., & Green, M. A. (1993, May). A new method for accurate measurements of the lumped series resistance of solar cells. In *Photovoltaic Specialists Conference, 1993., Conference Record of the Twenty Third IEEE* (pp. 133-139). IEEE.

[11] Castaner, L. and Silvestre, S. (2002). *Modelling photovoltaic systems using PSpice*. John Wiley and Sons.

[12] Nakajima, K., & Usami, N. (Eds.). (2009). *Crystal growth of Si for solar cells* (Vol. 97). Sendai, Japan: Springer.

[13] López, G., Ortega, P. R., Martín, I., Voz, C., Morales, A. B., Orpella, A., & Alcubilla, R. (2015). Base contacts and selective emitters processed by laser doping technique for p-type IBC c-Si solar cells. *Energy Procedia*, *77*, 752-758.

[14] López Rodríguez, G. (2016). Interdigitated back-contacted (IBC) c-Si solar cells based on laser processed dielectric layers.

[15] Silvestre S., Sentis L., Castaner L.. (1999). A fast low-cost solar cell spectral response measurement system with accuracy indicator. IEEE Transactions on instrumentation and measurement 48 (5), 944-948.

[16] Silvestre S., Guasch D., Ortega P and Calatayud R. (2004). Photovoltaic systems modelling using Matlab and Simulink. Proc. of the 19th European photovoltaic solar energy conference. 2207-2210.

[17] Silvestre S. Chapter IIA-4 – Review of System Design and Sizing Tools. (2012) In Practical handbook of photovoltaics: fundamentals and applications (second edition) Elsevier. 673-694.